This is to certify that the

thesis entitled
An Automated Procedure for Contact
Problems With and Without Frictional Effects
Utilizing the Boundary Integral Method

presented by

Glen Curtis Bennett II

has been accepted towards fulfillment
of the requirements for

Master's degree in Mechanics

Nicholas J Altiero

Major professor

Date November 7, 1988

AN AUTOMATED PROCEDURE FOR CONTACT PROBLEMS WITH AND WITHOUT FRICTIONAL EFFECTS UTILIZING THE BOUNDARY INTEGRAL METHOD

By

Glen Curtis Bennett II

A THESIS

Submitted to
Michigan State University
in partial fulfillment of the requirements
for the degree of

MASTER OF SCIENCE

Department of Metallurgy, Mechanics and Materials Science

1988

ABSTRACT

AN AUTOMATED PROCEDURE FOR CONTACT PROBLEMS WITH AND WITHOUT FRICTIONAL EFFECTS UTILIZING THE BOUNDARY INTEGRAL METHOD

By

Glen Curtis Bennett II

An automated incremental formulation for the solution of contact problems with and without frictional effects is presented. The formulation in this paper is restricted to isotropic, linear elastic materials. The formulation uses a static procedure to solve problems in the realm of small displacement theory but, with modification, the incremental algorithms can be expanded to handle problems within the area of large displacements. The numerical procedure employs a direct Boundary Integral formulation utilizing linear displacement interpolation functions and constant traction interpolation functions. This "mixed" formulation allows the modeling of traction discontinuities without involving supplemental equations.

ACKNOWLEDGMENTS

The author wishes to express his sincere appreciation for the help and support of his advisor, Dr. Nicholas J. Altiero, whose persistence during the course of a five year period allowed me to finish this thesis.

The support of this work by Garrett Turbine Engine Company, Phoenix, Arizona is most gratefully acknowledged.

The author also wishes to express his appreciation to his mother and father for all their support throughout his college career and to the rest of his family for their support and motivation that allowed him to complete his graduate course work.

Finally the author wishes to say thank you to Jim and Jean Eddy for the use of their computer equipment and knowledge which allowed him to type his thesis.

TABLE OF CONTENTS

PAGE

LIST OF TABLES

LIST OF FIGURES

INTRODUCTION

The analysis of structural systems in contact is of major importance to engineers. The contact of objects has two major effects: the transfer of load from one body to another and in most cases, high stress gradients in the areas of contact. Systems of this type include bearings, gear teeth, tires, turbine blade roots, and punches contacting sheet metal during metal forming processes. The analysis of these contact systems becomes more important as engineers try to simulate complex structures and how they interact with their surroundings.

The first to examine and solve contact problems was Hertz [1], in 1895. Hertz's studies assumed that tangential forces could be neglected and that the only forces transmitted from one body to another are normal forces. These assumptions imply that the contact is frictionless. A typical application which can be simulated by a frictionless model are ball and roller bearing problems. Based on the work of Hertz, handbooks were developed that gave the contact area and stress, for a given applied load. One such book was published in 1963 by Lipson and Juvinall [2]. This type of procedure, using simplified analytical methods to generate tables that could be adapted to similar problems, was used widely until numerical techniques were developed on digital computers. Other work in the area of contact problems has occurred since, but existing analytical solutions are restricted to relatively simple geometries and loading conditions and have rather limited engineering application.

To solve problems of practical interest, numerical techniques have been adopted to solve the problem of contact between elastic bodies. These numerical techniques allow the analyst to calculate values of interest, e.g.

1. pressure distribution in the contact region,
2. size of the contact area,
3. stresses near the contact area,
4. final deformed shapes of the bodies in contact.

The most widely used numerical technique for simulation of bodies in contact is the finite element method (FEM). When using the finite element approach, the total domain of the body is discretized and, in the contact region, special interface elements (gap elements) are used. The interface elements are made up of nodes on each body that are assumed to come into contact. The distance (gap) between a node on one body and the corresponding node on the second body is then measured by the interface element. When the two surfaces come into contact, the contact conditions are imposed [3]. In the region of contact, a fine mesh is required to predict the values of interest accurately. This can be done by using a fine mesh in the contact area and then propagating this fine mesh throughout the interior. This can cause the total system of equations to become large and computationally expensive to solve. The user may also refine the mesh in the area of contact and use multipoint constraints, which introduce master and slave degrees of freedom, to help transition the mesh from fine to coarse. Other transitioning techniques can also be employed, but in general this means increased degrees of freedom or the introduction of constraint equations. These refinement techniques allow for the accurate simulation of the displacement in the contact region. The only other special consideration that

needs to be given to the analysis of contact problems is the nonlinearities that arise due to the contact between multiple bodies. These nonlinearities are simulated using incremental techniques that approximate nonlinear behavior in a piecewise linear manner. This type of procedure is common when finite element analysis is used to simulate nonlinear behavior.

Fredriksson, in 1976 [4], proposed a procedure using a finite element approach based on an iterative incremental procedure. His emphasis was on the development of a slip criterion and an associated slip rule for contact with friction. Fredriksson also suggested the use of a superelement approach which would produce a more computationally efficient iterative technique because only the superelement which contained the contact region would be updated each iteration. Mahmoud, Salamon and Marks in 1982 [5], developed a numerical method to provide user convenience, simplify user input, and make the solution of bodies in contact more computationally efficient by eliminating the iterative portion of the contact procedure. Using the theory of linear elasticity, they automated the finite element method to obtain the extent of contact versus the load increment. Their program dealt with advancing contact problems without friction. Maxurkiewicz and Ostachowicz, in 1983 [6], used spring-like interface elements to predict rigid contact, sliding, and rigid body motion within the contact region. Torstenfelt wrote papers in 1983 and 1984 [7,8] based on a finite element formulation which utilized only stiffness equations, i.e. no gap elements. His procedure treated the tangential forces as known quantities, and calculated them from the previous load step. His second paper used an algorithm that scaled the applied load to introduce only one change of contact status in each

load step. This allows the numerical procedure to be linear between discrete contact points. In 1984, Rahman, Cook, and Wilkinson [9] developed a technique without special interface elements that could be easily extended to multiple contact surface problems. Their program used multiple iteration requirements in the contact region to control the convergence criterion. Many other papers have been written using numerical procedures based on the finite element method, using special interface elements, flexibility formulations, stiffness equations only, or combinations of all three. Most apply a load increment and iterate based upon a convergence criterion. This criterion may be based upon contact conditions remaining constant for more than one iteration or equilibrium considerations that sum forces (internal and external) until a tolerance level is reached. However, with both the boundary and the interior discretized, as done with a finite element formulation, this iterative process can become computationally uneconomical.

In the solution of a contact problem, the boundary region in contact is of primary importance. This would indicate that a numerical solution which involves discretization of only the boundary might be a preferable approach. A numerical technique of this type would be the boundary element method (BEM) [10,11]. Work has been done on the application of the BEM to contact problems, notably papers by Andersson [12,13], which explored the use of constant, linear and parabolic boundary elements. Andersson's first paper dealt with two-dimensional contact problems with frictional forces. His approach used constant interpolating functions for the displacements and tractions. The analysis assumes the conditions for adhesion, slip, and the direction of the frictional forces for each load step. These conditions are then checked after the load step has been applied. If the assumptions are correct, then the next load increment

can be applied. If the assumptions are wrong, new conditions are chosen and the analysis is repeated. This iterative procedure is followed until the correct contact conditions are found and the analysis is completed. Andersson's second paper explored the use of linear and quadratic boundary elements to solve two-dimensional problems of bodies in contact with friction. Abdul-Mihsein, Bakr and Parker [14] stated that the Boundary Element Method is well-suited for analysis of bodies in contact because the tractions are calculated with the same accuracy as the displacements. Their analysis of frictionless contact problems used an automated incremental procedure to solve axisymmetric problems. This procedure used quadratic elements with an automated incremental technique, exploiting linear elasticity and small deformation theory, to solve problems involving bodies in contact.

In this thesis, the contributions of these authors are brought together. The intention is to assemble the best techniques, simplify, automate, and more accurately simulate bodies in contact. The numerical form of the boundary integral formulation presented will be different than those discussed earlier, in that the order of the interpolating functions will be linear for the displacements and constant for the tractions. This will allow the simulation of corners and discontinuous loading on the boundary in a straight-forward manner. This differs from other formulations which use the same order of interpolation functions for both the displacements and tractions. The present formulation will be applied to frictionless and frictional contact problems using an automated incremental technique. The emphasis will be to handle contact problems within the realm of small displacement theory and linear elasticity.

CHAPTER II

BOUNDARY ELEMENT THEORY

II.1 DERIVATION OF THE BOUNDARY INTEGRAL EQUATIONS

This chapter contains the formulation of the boundary element method as it applies to plane boundary-value problems in elastostatics. The first section contains the derivation of the boundary integral equations from the reciprocal work theorem. In the second section, the derived integral equations are applied to plane boundary-value problems of elastostatics. The third section contains the numerical procedure employed to implement the boundary integral equations via a general computer program. The last section contains the logic used in the current computer program to solve plane boundary- value problems.

The reciprocal work theorem as stated by Betti and Rayleigh is as follows:

> if an elastic body is subjected to two different systems of external forces, then the work that would be done by the first system of external forces acting through the displacements associated with the second system of forces is equal to the work that would be done by the second system of forces acting through the displacements associated with the first system of forces [20].

If the two equilibrium states (X_i, t_i, u_i) and (X_i^*, t_i^*, u_i^*) exist in the region R bounded by B then by the reciprocal work theorem the following equation can be written:

$$\int_B t_i^*(\underline{x})u_i(\underline{x})ds(\underline{x}) + \int_R X_i^*(\underline{x})u_i(\underline{x})da(\underline{x}) = \int_B t_i(\underline{x})u_i^*(\underline{x})ds(\underline{x}) + \int_R X_i(\underline{x})u_i^*(\underline{x})da(x), \tag{II.1}$$

where

X_i = components of the body force vector,

t_i = components of the boundary traction vector,

u_i = components of the displacement vector,

ds = a differential length on the boundary B,

da = a differential area in the domain R,

and summation over repeated indices is inferred. Next, let us choose the set of displacements, tractions, and body forces (X_i^*, t_i^*, u_i^*) to be those associated with a unit excitation at $\underline{x}=\underline{\zeta}$ in an infinite plane, i.e.

$$\begin{aligned} X_i^* &= \delta(\underline{x} - \underline{\zeta})e_i(\underline{\zeta}), \\ u_i^* &= (uR)_{ij}(\underline{x},\underline{\zeta})e_j(\underline{\zeta}), \\ t_i^* &= (tR)_{ij}(\underline{x},\underline{\zeta})e_j(\underline{\zeta}), \end{aligned} \tag{II.2}$$

where

$(tR)_{ij}(\underline{x},\underline{\zeta})$ = the traction, $t_i(\underline{x})$, due to a unit force, $R_j(\underline{\zeta})$, applied in the infinite elastic plane,

$(uR)_{ij}(\underline{x},\underline{\zeta})$ = the displacement, $u_i(\underline{x})$,due to a unit force, $R_j(\underline{\zeta})$, applied in the infinite elastic plane,

$\delta(\underline{x}-\underline{\zeta})$ = dirac delta function representing a disturbance at $\underline{x}=\underline{\zeta}$,

$e_i(\zeta)$ = unit direction vector.

The functions $(tR)_{ij}(\underline{x},\underline{\zeta})$ and $(uR)_{ij}(\underline{x},\underline{\zeta})$ are called influence functions and are given in Appendix A. When Equations (II.2) are substituted into Equation (II.1) the resulting equation becomes

$$e_j(\zeta)\int_B (tR)_{ij}(\underline{x},\underline{\zeta})\,u_i(\underline{x})\,ds(\underline{x}) + e_i(\zeta)\int_R \delta(\underline{x}-\underline{\zeta})\,u_i(\underline{x})\,da(\underline{x}) =$$

$$e_j(\zeta)\left[\int_B (uR)_{ij}(\underline{x},\underline{\zeta})\,t_i(\underline{x})\,ds(\underline{x}) + \int_R (uR)_{ij}(\underline{x},\underline{\zeta})X_i(\underline{x})\,da(\underline{x})\right]. \qquad \text{(II.3)}$$

The second term on the left hand side can be simplified as follows:

$$e_i(\zeta)\int_R \delta(\underline{x}-\underline{\zeta})\,u_i(\underline{x})\,da(\underline{x}) = e_i(\zeta)u_i(\zeta)$$
$$= e_j(\zeta)u_j(\zeta),$$

provided that ζ is in the domain R bounded by B. Equating coefficients of $e_j(\zeta)$ from equation (II.3), the following equations are obtained:

$$u_j(\zeta) = -\int_B (tR)_{ij}(\underline{x},\underline{\zeta})\,u_i(\underline{x})\,ds(\underline{x}) + \int_B (uR)_{ij}(\underline{x},\underline{\zeta})\,t_i(\underline{x})\,ds(\underline{x}) +$$

$$\int_R (uR)_{ij}(\underline{x},\underline{\zeta})X_i(\underline{x})\,da(\underline{x}). \qquad \text{(II.4)}$$

It can be seen from the list of influence functions in Appendix A that if the symbols $\underline{x}$ and $\underline{\zeta}$ are interchanged the following are true:

$$(uR)_{ji}(\zeta,\underline{x}) = (uR)_{ji}(\underline{x},\zeta) = (uR)_{ij}(\underline{x},\zeta)$$

$$(tR)_{ji}(\zeta,\underline{x}) = -(tR)_{ji}(\underline{x},\zeta), \tag{II.5}$$

provided that $n_i = n_i(\zeta)$, where $\underline{n}$ is a unit normal vector to a plane at ζ. This yields

$$u_i(\underline{x}) = \int_B (tR)_{ji}(\underline{x},\zeta)u_j(\zeta)ds(\zeta) + \int_B (uR)_{ij}(\underline{x},\zeta)\, t_j(\zeta)ds(\zeta) + \int_R (uR)_{ij}(\underline{x},\zeta)X_j(\zeta)da(\zeta), \tag{II.6}$$

where i = 1,2 and $\underline{x}$ is in the domain R. Equations (II.6) can be used to solve for the displacements anywhere in the domain R given a complete set of boundary information and are known as the field equations.

The boundary equation can be developed from Equation (II.6) by taking the point $\underline{x}$ to the boundary B. If Equation (II.6) is applied to a point $\underline{x}$ on B then special consideration is needed as $\zeta \rightarrow \underline{x}$ since the integrands become singular. The influence function $(tR)_{ji}(\underline{x},\zeta)$ varies as $1/\rho$ and the influence function $(uR)_{ij}(\underline{x},\zeta)$ varies as $\ln(\rho)$, where ρ is the distance between the source point ζ and the field point $\underline{x}$, i.e.

$$\rho = [(x_1 - \zeta_1)^2 + (x_2 - \zeta_2)^2]^{1/2}.$$

See appendix A for a listing of the influence functions $(tR)_{ji}$ and $(uR)_{ij}$. Although the integrands containing $(uR)_{ij}(\underline{x},\zeta)$ are singular, the integrals are definite and pose no problem. The integrand containing $(tR)_{ji}(\underline{x},\zeta)$ is also singular and the

integral is undefined as $\underline{x} \rightarrow \underline{\zeta}$. To avoid this singularity, the integration path is taken on a semicircle of radius ε around the point of singularity, and the limit of the integral as $\varepsilon \rightarrow 0$ is calculated (see Figure II.1).

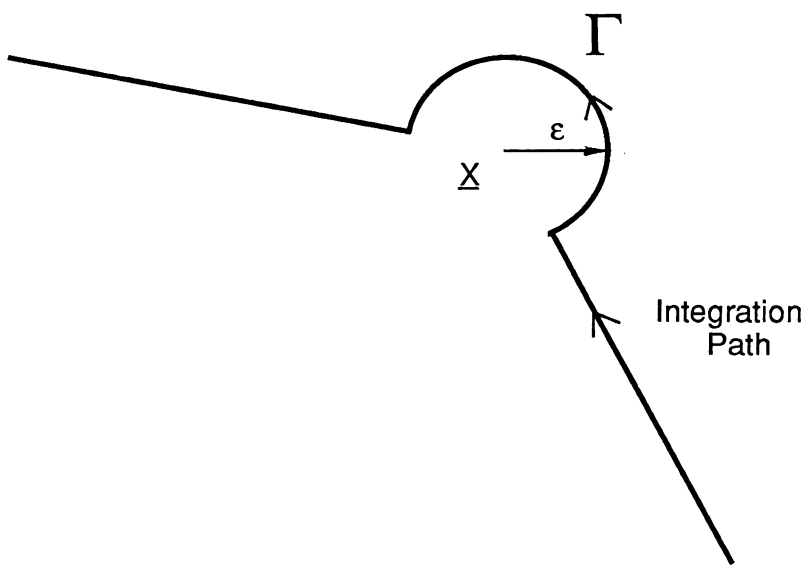

Figure II.1

The integration path around the point of singularity.

Thus,

$$\int_B (tR)_{ji}(\underline{x},\underline{\zeta})u_j(\underline{\zeta})ds(\underline{\zeta}) = \lim_{\varepsilon\rightarrow 0}\int_\Gamma (tR)_{ji}(\underline{x},\underline{\zeta})u_j(\underline{\zeta})ds(\underline{\zeta}) +$$

$$-\int_B (tR)_{ji}(\underline{x},\underline{\zeta})u_j(\underline{\zeta})ds(\underline{\zeta}), \qquad (II.7)$$

where the second integral on the right is the integral contribution for the entire boundary except at the point of singularity and is known as a Cauchy principal-value integral. Equation (II.6) can now be written as:

$$u_i(\underline{x}) = \beta_{ji}u_j + \int\!\!\!\!\!\!-_B (tR)_{ji}(\underline{x},\zeta)u_j(\zeta)ds(\zeta) + \int_B (uR)_{ij}(\underline{x},\zeta)\, t_j(\zeta)ds(\zeta) +$$

$$\int_R (uR)_{ij}(\underline{x},\zeta)X_j(\zeta)da(\zeta), \qquad \text{(II.8)}$$

where

$$\beta_{ji} = \lim_{\varepsilon\to 0} \int_\Gamma (tR)_{ji}(\underline{x},\zeta)u_j(\zeta)ds(\zeta).$$

The left-side of equation (II.8) can be written as:

$$u_i(\underline{x}) = \delta_{ji}u_j(\underline{x}),$$

where $\alpha_{ji}(\underline{x}) = \delta_{ji} - \beta_{ji}$ and Equation (II.8) becomes

$$\alpha_{ji}(\underline{x})u_j(\underline{x}) - \int\!\!\!\!\!\!-_B (tR)_{ji}(\underline{x},\zeta)u_j(\zeta)ds(\zeta) = \int_B (uR)_{ij}(\underline{x},\zeta)\, t_j(\zeta)ds(\zeta) +$$

$$\int_R (uR)_{ij}(\underline{x},\zeta)X_j(\zeta)da(\zeta), \qquad \text{(II.9)}$$

where $\underline{x}$ is on B. The derivation of the free term α_{ji} is given in Appendix B. Before proceeding, it should be noted that the following influence functions are simular:

$$(tR)_{ji}(\underline{x},\zeta) = -(uc)_{ij}(\underline{x},\zeta),$$

where

$(uc)_{ij}(\underline{x},\zeta)$ = the displacement, $u_i(\underline{x})$, due to a unit displacement discontinuity, $c_j(\zeta)$, applied in the infinite elastic plane.

II.2 BOUNDARY ELEMENT FORMULATION

Consider a plane linear elastic region R, with boundary B, supported and loaded in some manner, as shown in Figure II.2.

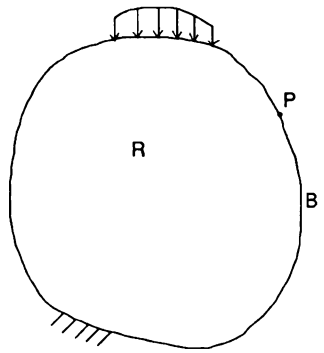

Figure II.2

Boundary-Value problem in plane elasticity.

Now Equation (II.9) can be rewritten as:

$$\alpha'_{ij}(\underline{x})u_j(\underline{x}) + \int_B (uc)_{ij}(\underline{x},\underline{\zeta})u_j(\underline{\zeta})ds(\underline{\zeta}) = \int_B (uR)_{ij}(\underline{x},\underline{\zeta})\, t_j(\underline{\zeta})ds(\underline{\zeta}) \qquad (II.10)$$

where the body force term has been set to zero. This is called Somigliana's identity, which relates the displacements and tractions at any point P=$\underline{x}$ on B to all tractions and displacements on the boundary. Equation (II.10) is equivalent to Equation (II.9) but has a more straightforward physical interpretation for the term $(uc)_{ij}$ [22].

Equations (II.10) are valid for all $\underline{x}$ on B, where

B = the boundary enclosing the region R,

$\underline{x}$ = field point,

$\underline{\zeta}$ = source point,

s = distance measured along the boundary,

t_i = components of the traction vector,

u_i = components of the displacement vector,

$(uc)_{ij}$ = influence function for a unit displacement discontinuity applied in an infinite elastic plane,

$(uR)_{ij}$ = influence function for a unit force applied in an infinite elastic plane,

α'_{ij} = the contribution of the integral around the singularity point, called the free term.

A list of the influence functions $(uc)_{ij}$ and $(uR)_{ij}$ are in Appendix A. For every point on the boundary, either the traction or displacement is known in a given direction. Equation (II.10) is used to solve for all unknown boundary information, thus giving a complete set of known boundary tractions and displacements. Then at any point $\underline{x}$ in R the displacements can be calculated from the equation:

$$u_i(\underline{x}) = \int_B (uR)_{ij}(\underline{x},\underline{\zeta})\, t_j(\underline{\zeta})\, ds - \int_B (uc)_{ij}(\underline{x},\underline{\zeta})\, u_j(\underline{\zeta})\, ds, \qquad \text{(II.11)}$$

which was developed in the previous section for any point $\underline{x}$ in the domain R. From equations (II.11), equations can be formed that will allow the stresses anywhere in the domain R to be calculated, provided that a complete set of tractions and displacements are known on the boundary. This is done by

applying the plane stress version of Hooke's law to Equation (II.11). Hooke's law states:

$$\sigma_{11} = (2G/(1 - \nu))(u_{1,1} + \nu u_{2,2}),$$
$$\sigma_{22} = (2G/(1 - \nu))(u_{2,2} + \nu u_{1,1}),$$
$$\sigma_{12} = G(u_{1,2} + u_{2,1}), \qquad \text{(II.12)}$$

where G is the shear modulus and ν is Poisson's ratio. If Equations (II.12) are applied to Equations (II.11) then the results are:

$$\sigma_{ik}(\underline{x}) = \int_B (\sigma R)_{ikj}(\underline{x},\zeta)\, t_j(\zeta) ds - \int_B (\sigma c)_{ikj}(\underline{x},\zeta)\, u_j(\zeta) ds, \qquad \text{(II.13)}$$

where

σ_{ik} = components of the stress tensor,

$(\sigma R)_{ikj}(\underline{x},\zeta)$ = stress component, $\sigma_{ik}(\underline{x})$, due to a unit force, $R_j(\zeta)$, applied in an infinite plane,

$(\sigma c)_{ikj}(\underline{x},\zeta)$ = stress component, $\sigma_{ik}(\underline{x})$, due to a unit displacement discontinuity, $c_j(\zeta)$, applied in an infinite plane.

Equations (II.11) and (II.13) relate the boundary tractions and displacements to the internal displacements and stresses anywhere in the domain R. A list of the influence functions $(\sigma c)_{ikj}$ and $(\sigma R)_{ikj}$ are given in Appendix A.

II.3 NUMERICAL PROCEDURE

Since Somigliana's identity can only be solved for simple geometries with simple traction and displacement boundary conditions, the boundary B is broken into N segments (see Figure II.3).

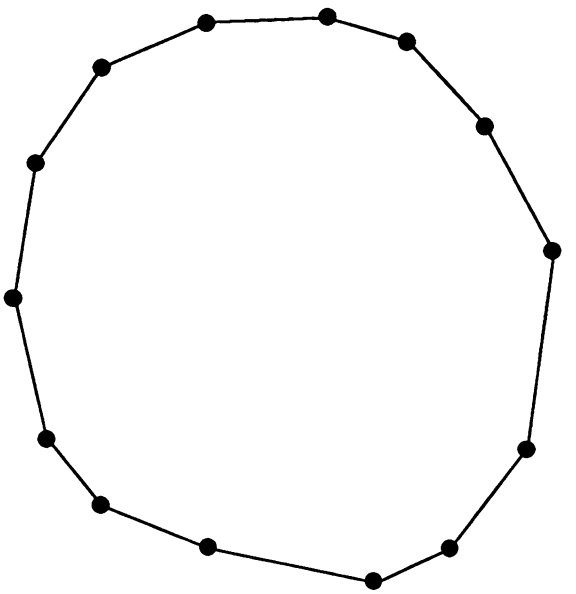

Figure II.3

Complex geometry broken into segments (boundary elements).

Over each segment, approximate functions to the actual variations of the displacements and tractions are chosen. The integral over the entire boundary B then becomes a summation of the N integrals over the individual segments. Thus Equations (II.10) become

$$\alpha'_{ij}(\underline{x}^n)u_j(\underline{x}^n) + \sum_{m=1}^{N}\int_m (uc)_{ij}(\underline{x}^n,\underline{\zeta})u_j(\underline{\zeta})ds = \sum_{m=1}^{N}\int_m (uR)_{ij}(\underline{x}^n,\underline{\zeta})\, t_j(\underline{\zeta})ds \qquad (II.14)$$

where $\underline{x}^n$, represents a segment endpoints. The variation for the displacements and tractions can be constant, linear, parabolic or of higher order forms. The numerical procedure developed for this thesis uses a linear variation for the displacement function and a constant variation for the traction function over each

segment. The formulation of constant tractions and linear displacements is emphasized here because it allows the model to have discontinuous tractions and also allows the modeling of corners without any special considerations. This differs from the formulations which appear in the literature, where:

> ... although displacements at a corner node can be specified unambiguously, the specified tractions can only be represented by considering two corner nodes indefinitely close to each other (typically 0.005 times the length of the local boundary element apart) representing the limiting endpoints of the two surfaces [16].

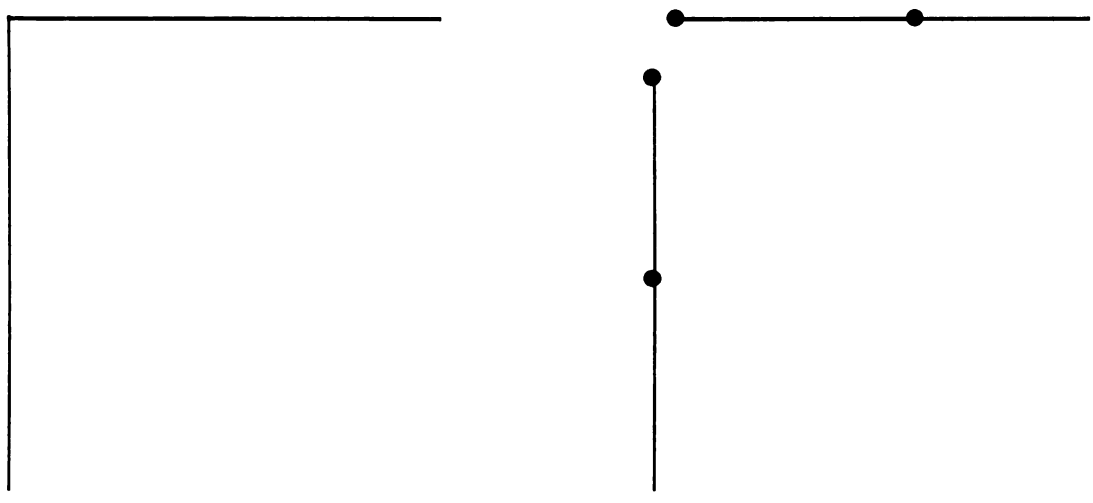

Figure II.4

The actual corner (left) is modeled using two corner nodes (right) with typical BEM formulations.

A further discussion on the use of linear displacement and constant traction functions is given in Appendix D.

To simplify the integration over each segment further, shape functions are introduced to approximate the variation of the displacements over each segment (boundary element), i.e.

$$u_j = u_j^{m-1}N_1(\xi) + u_j^m N_2(\xi),$$

$$t_j = t_j^m$$

$$N_1(\xi) = .5(1-\xi),$$

$$N_2(\xi) = .5(1+\xi),$$

$$ds = .5(s_m - s_{m-1})d\xi = .5\Delta s_m d\xi,$$

where

u_j^{m-1} = the displacement at the beginning point of element m,

u_j^m = the displacement at the end point of element m,

ξ = local coordinate that varies from -1 to 1,

N_i = shape functions,

Δs_m = length of element m.

Thus Equations (II.14) become:

$$2\alpha'_{ij}(\underline{x}^n)u_j^n + \sum_{m=1}^{N}\Delta s_m\Big[u_j^{m-1}\int_m (uc)_{ij}(\underline{x}^n,\xi)N_1(\xi)d\xi + u_j^m\int_m (uc)_{ij}(\underline{x}^n,\xi)N_2(\xi)d\xi\Big] = \sum_{m=1}^{N}\Delta s_m t_j^m\int_m (uR)_{ij}(\underline{x}^n,\xi)d\xi, \qquad (II.15)$$

where t_j^m is the value of the traction component on element m. This can be written in a simpler form as

$$2\alpha'_{ij}(\underline{x}^n)u_j^n + \sum_{m=1}^{N}\Big[A_{ij}^{mn}u_j^{m-1} + B_{ij}^{mn}u_j^m\Big] = 1/G\sum_{m=1}^{N}C_{ij}^{mn}F_j^m, \qquad (II.16)$$

where

$$A_{ij}^{mn} = \Delta s_m \int_m (uc)_{ij}(x^n,\xi) N_1(\xi)\, d\xi,$$

$$B_{ij}^{mn} = \Delta s_m \int_m (uc)_{ij}(x^n,\xi) N_2(\xi)\, d\xi,$$

$$C_{ij}^{mn} = G \int_m (uR)_{ij}(x^n,\xi)\, d\xi,$$

$$F_j^m = \Delta s_m t_j^m.$$

Note that the integrands of A_{ij}^{mn} and B_{ij}^{mn} are singular when m=n or m=n+1. This is the case for the element that begins or ends with the node n (see Figure II.5).

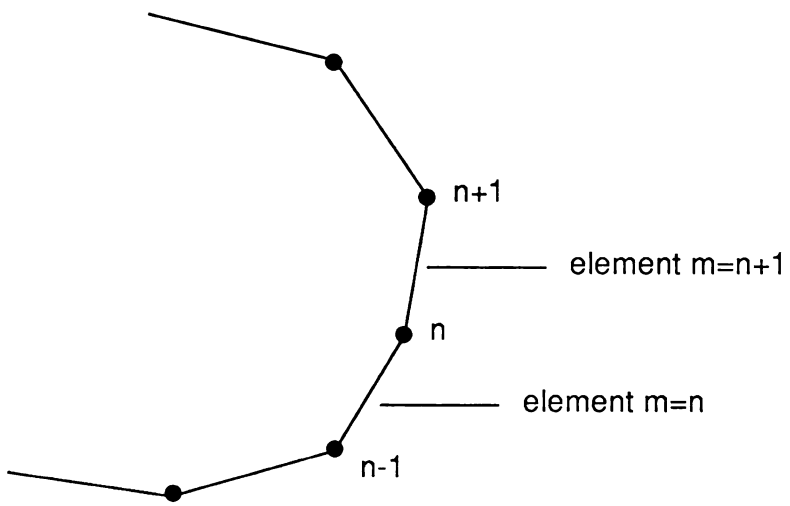

Figure II.5

Partial diagram of the boundary showing the boundary elements with singular considerations.

The singular integrals are evaluated analytically while all other nonsingular integrals are evaluated by numerical integration using a Guass quadrature formulation. A list of the solutions for the singular integrals are in Appendix E.

II.4 COMPUTER IMPLEMENTATION

The computer program is based on the numerical procedure developed in the previous section. First the coefficient matrices [uc] and [uR] are formed from the boundary coordinates and material information. Equation (II.16) expressed in matrix form becomes

$$[uc]G\{u\} = [uR]\{F\} .$$

This system of equations relates nodal displacements to resultant segment forces. To create a well-posed problem relating nodal displacements to nodal forces, a transformation is required. If we let the nodal force be given by

$$\mathbf{F}_i^m = .5\,[F_i^m + F_i^{m+1}] ,$$

then a transformation matrix can be written such that :

$$\{\mathbf{F}\} = [T]\,\{F\} , \qquad \text{(II.17)}$$

where

$$[T] = .5 \begin{bmatrix} 1 & 1 & 0 & 0 & \cdot & 0 \\ 0 & 1 & 1 & 0 & \cdot & 0 \\ 0 & 0 & 1 & 1 & \cdot & 0 \\ 0 & 0 & 0 & 1 & \cdot & 0 \\ \cdot & \cdot & \cdot & \cdot & \cdot & \cdot \\ 1 & 0 & 0 & 0 & \cdot & 1 \end{bmatrix} ,$$

and I is the 2x2 identity matrix,

$$I = \begin{bmatrix} 1 & 0 \\ 0 & 1 \end{bmatrix} .$$

If both sides of Equation (II.17) are multiplied by $[T]^{-1}$ then the following equation is formed:

$$[T]^{-1}\{\mathbf{F}\} = \{F\}$$

and

$$[uc]\, G\, \{u\} = [uR]\, [T]^{-1}\{\mathbf{F}\}, \qquad \text{(II.18)}$$

where

$$[T]^{-1} = \begin{bmatrix} I & -I & I & -I & \cdot & I \\ I & I & -I & I & \cdot & -I \\ -I & I & I & -I & \cdot & I \\ I & -I & I & I & \cdot & -I \\ \cdot & \cdot & \cdot & \cdot & \cdot & \cdot \\ -I & I & -I & I & \cdot & I \end{bmatrix}$$

provided that the number of nodes is odd. The next step in the computer program is to post multiply the matrix [uR] by the inverse of the transformation matrix. Now our system of equations is as follows:

$$[uc]\, G\, \{u\} = [M]\, \{\mathbf{F}\}, \qquad \text{(II.19)}$$

where

$$[M] = [uR]\,[T]^{-1}.$$

To insure equilibrium on the system of equations, a set of supplemental equations are augmented to the system. The three supplemental equations are:

1. The summation of forces in the X direction, i.e.

$$\sum_{i=1}^{N} \mathbf{F}_1^i = 0,$$

2. The summation of forces in the X_2 direction, i.e.

$$\sum_{i=1}^{N} \mathbf{F}_2^i = 0,$$

3. The summation of moments about node 1, i.e.

$$\sum_{i=1}^{N} (X_1 \mathbf{F}_2^i - X_2 \mathbf{F}_1^i) = 0.$$

In matrix form, these can be expressed as,

$$[Q]\,\{\mathbf{F}\} = \{0\},$$

where

$$[Q] = \begin{bmatrix} 1 & 0 & 1 & 0 & \cdots & 1 & 0 \\ 0 & 1 & 0 & 1 & \cdots & 0 & 1 \\ 0 & 0 & x_2^1-x_2^2 & x_1^2-x_1^1 & \cdots & x_2^1-x_2^N & x_1^N-x_1^1 \end{bmatrix}$$

and the system of equations becomes

$$\begin{bmatrix} [uc] & -[Q]^T \\ [O] & [O] \end{bmatrix} \begin{bmatrix} G\{u\} \\ \{\lambda\} \end{bmatrix} = \begin{bmatrix} [M] \\ [Q] \end{bmatrix} \begin{bmatrix} \{F\} \end{bmatrix} \qquad \text{(II.20)}$$

where $\{\lambda\}$ is a small perturbation (equilibrium residuals) which should approach zero as $N \rightarrow \infty$. Equation (II.20) contains both unknown displacements and unknown tractions, so to set up a system of equations that can be solved for the unknowns, Equation (II.20) must be rearranged. All unknown forces and the coefficients that multiply them are moved from the right hand side of Equation (II.20) to the left hand side of Equation (II.20). The corresponding known displacements and the coefficients that multiply them are moved to the right hand side of Equation (II.20). Once all unknown quantities are in the left hand side vector and all known quantities are in the right hand side vector, the two matrices on the right hand side are multiplied together to produce a column matrix of real numbers. The system of equations now looks like,

$$[A]\{x\} = \{B\}, \qquad \text{(II.21)}$$

where

$\{x\}$ = unknown tractions, displacements and three λ_i terms, that are related to the equilibrium equations,

$[A]$ = the coefficients of [uc] and modified [uR] that multiply the unknown matrix $\{x\}$,

$\{B\}$ = the resultant of the matrices that were multiplied together.

Equation (II.21) can now be solved for the matrix {x} of unknown quantities. When the results for {x} are obtained, a complete set of boundary information is known. From the complete set of boundary information, displacements and stresses anywhere in the domain R can be calculated from the numerical form of equations (II.11) and (II.13).

CHAPTER III

APPLICATION OF BOUNDARY ELEMENT METHOD TO CONTACT PROBLEMS

III.1 DESCRIPTION OF THE CONTACT PROBLEM

Two bodies are in contact when forces are transferred from one body to another through an area on the boundary of each body. Here, the contact area of body A in the deformed state is denoted C^A and the contact area of body B in the deformed state is denoted C^B. Each of these areas is a subset of an area denoted as the potential contact area for each body, $C^A_{potential}$ and $C^B_{potential}$, respectively. These potential contact areas are defined by the analyst before the simulation is started and should include areas larger than the expected contact areas. After all of the external load has been applied, the actual contact areas C^A and C^B will be subsets less than or equal to the potential contact areas of the two bodies. The contact region can also be classified as advancing or receding. An advancing contact region grows larger as the next load step is applied. A receding contact region shrinks as the next load step is applied. Thus in an advancing contact problem the initial contact area is less than the final contact region, and in a receding contact problem the initial contact area is greater than the final contact area.

When two bodies are in contact, nonlinearities are introduced into the system. The response of two bodies in contact will be nonlinear for various reasons. The first of these reasons is that the stiffness of the system is a function of the relative displacement between the two bodies. This concept of nonlinearity can be explained with the use of a simple example (see Figure III.1).

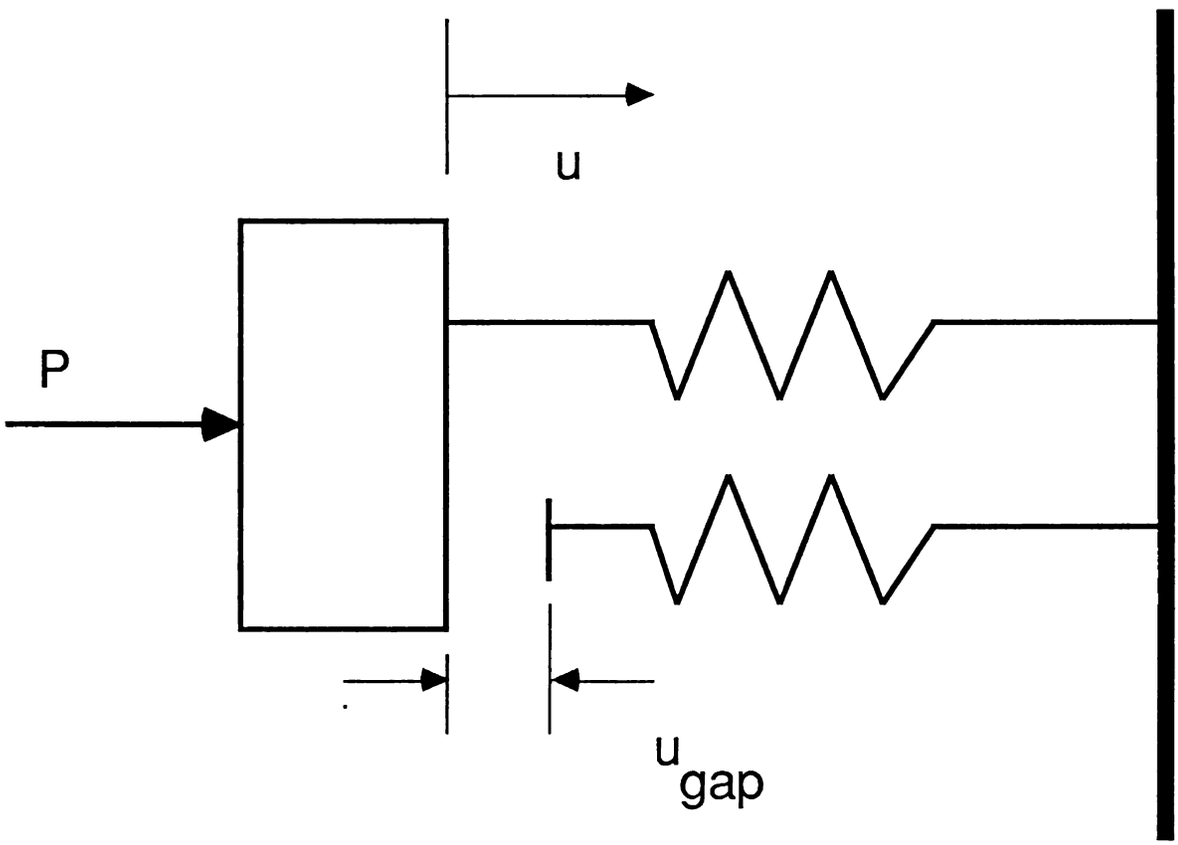

Figure III.1

Simple one degree of freedom system [21].

It can be seen that when the displacement becomes greater than the initial gap, the stiffness of the system will change abruptly (see Figure III.2).

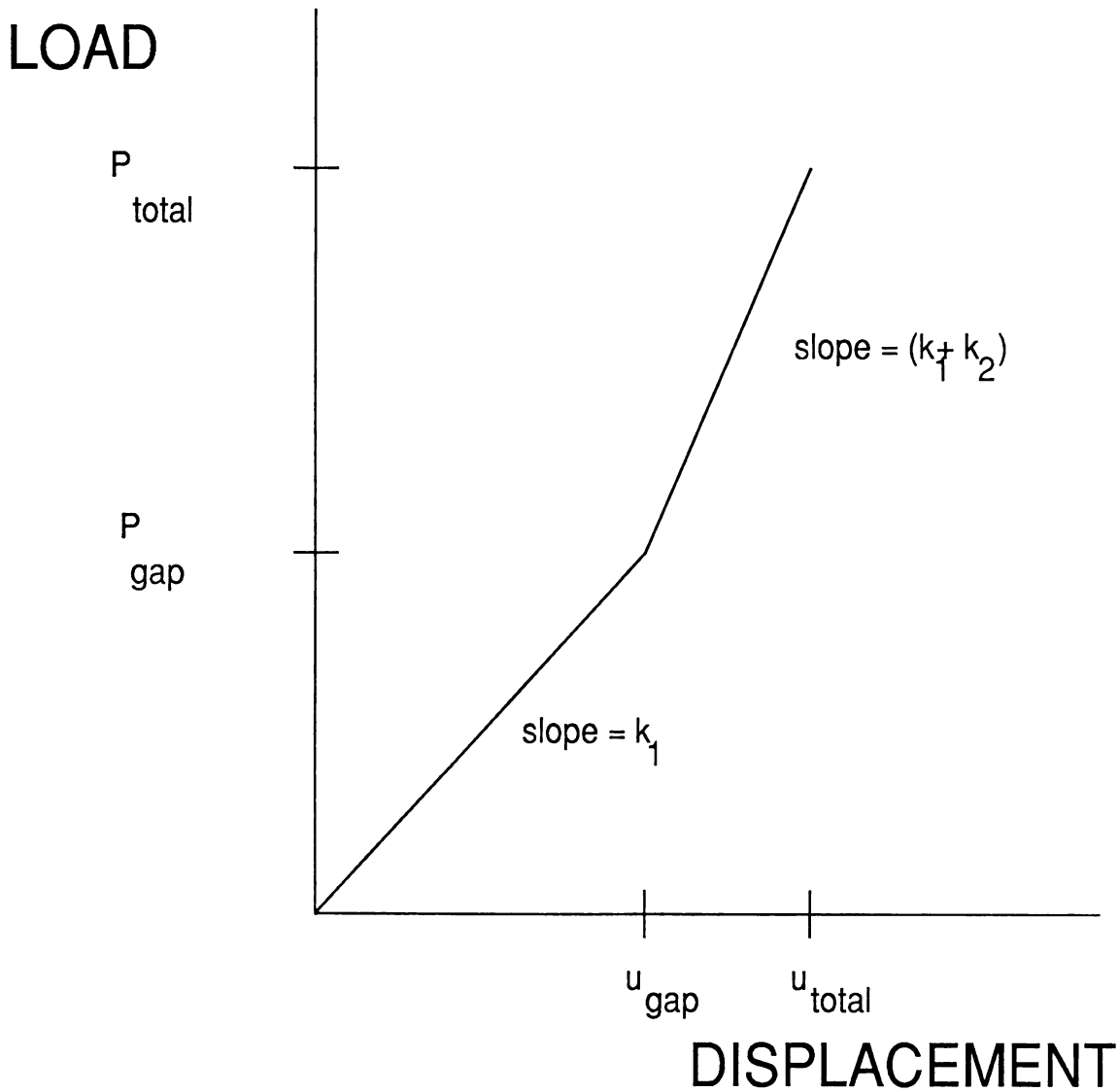

Figure III.2

Load-displacement diagram of the problem shown in Figure III.1 [21].

The nonlinearity of two bodies in contact can also be expressed in terms of the boundary conditions. During the loading of the system, the contact area can

expand or contract based on the relative displacement of the bodies in contact. This will change the force and displacement conditions within the contact region as the relative displacement (gap) of the two bodies changes. Therefore the force and displacement conditions in the contact region are a function of the displacement (see Figure III.3).

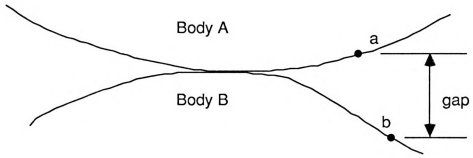

Figure III.3

Enlarged view of the contact zone.

This can be represented by the following equations which hold for a given increment of load, provided there is no slip:

$$\Delta t^a_i = 0 \qquad \text{gap} > 0$$
$$\Delta t^b_i = 0$$

$$-\Delta t^a_n = \Delta t^b_n \qquad \text{gap} = 0$$
$$-\Delta t^a_t = \Delta t^b_t \qquad \text{(III.1)}$$

$$\Delta u^a_n = \Delta u^b_n \qquad \text{gap} = 0$$
$$\Delta u^a_t = \Delta u^b_t$$

where the direction of the local coordinate system is defined in Figure III.9, and

Δt^a_i = components of the incremental traction vector for body A at node a in the global coordinate system,

Δt^b_i = components of the incremental traction vector for body B at node b in the global coordinate system,

Δt^a_n = normal component of the incremental traction vector for body A at node a in the local coordinate system normal to the boundary,

Δt^b_n = normal component of the incremental traction vector for body B at node b in a local coordinate system normal to the boundary,

Δt^a_t = tangential component of the incremental traction vector for body A at node a in a local coordinate system tangent to the boundary,

Δt^b_t = tangential component of the incremental traction vector for body B at node b in a local coordinate system tangent to the boundary,

Δu^a_n = normal component of the incremental displacement vector for body A at node a in a local coordinate system normal to the boundary,

Δu^b_n = normal component of the incremental displacement vector for body B at node b in a local coordinate system normal to the boundary,

Δu^a_t = tangential component of the incremental displacement vector for body A at node a in a local coordinate system tangent to the boundary,

Δu^b_t = tangential component of the incremental displacement vector for body B at node b in a local coordinate system tangent to the boundary.

Another nonlinear consideration is when friction is present in the contact region. When frictional forces are introduced into the system, the system becomes nonconservative and the final equilibrium state is path dependent. For these reasons the simulation of bodies in contact is a very complex problem and requires special numerical treatment.

As can be seen from Figure III.2, a problem in the numerical simulation can occur as the relative displacement closes the initial gap and a new contact status is achieved. To simulate this nonlinear environment the process is divided into m steps. Each of these m steps, if properly chosen, can be approximated by linear equations. This gives a stepwise linear approximation to a nonlinear analysis. If the contact, adhesion, and slip areas are constant throughout a load step, then the problem is numerically linear during that load step between discrete contact points. This type of incremental technique, when incorporated into numerical methods, allows the user to solve complex contact problems with and without friction. Incremental techniques will allow the simulation of nonlinear properties of the stiffness and boundary conditions discussed earlier, and incremental formulations will also allow the simulation of any irreversible frictional effects encountered in the contact region. An incremental technique for the solution of a contact problem would consist of six steps:

1. assemble the required matrices,
2. apply the external loads for the current load step,
3. solve the system of equations for unknown quantities,
4. update total displacement and traction quantities,
5. check to see if the total external loads have been applied
   A. YES go to step 6
   B. NO repeat steps 1-5,
6. calculate the stress quantities requested.

The incremental procedure applied to the contact problem of Figure III.4, with the basic assumptions of small displacements and linear elastic material behavior, would be as follows.

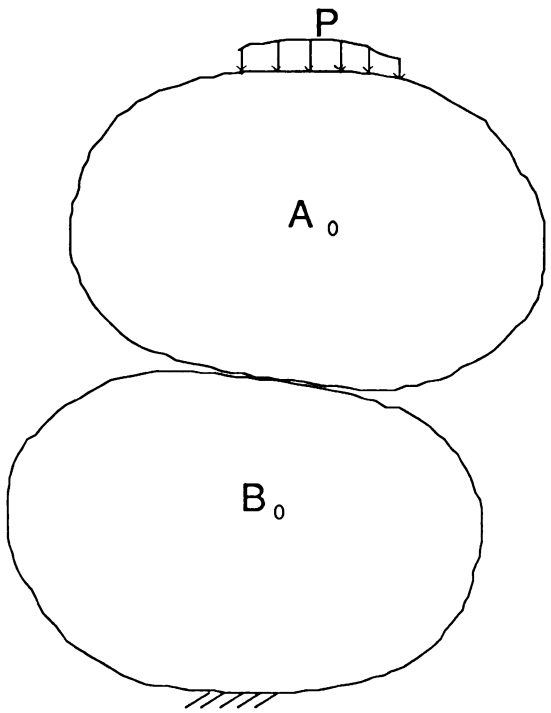

Figure III.4

Contact problem to be solved.

The externally applied load P is divided into m increments such that,

$$P_1 + P_2 + \cdots + P_m = P \,, \qquad \text{(III.3)}$$

where

P_k = the applied external load during load step k.

LOAD INCREMENT 1

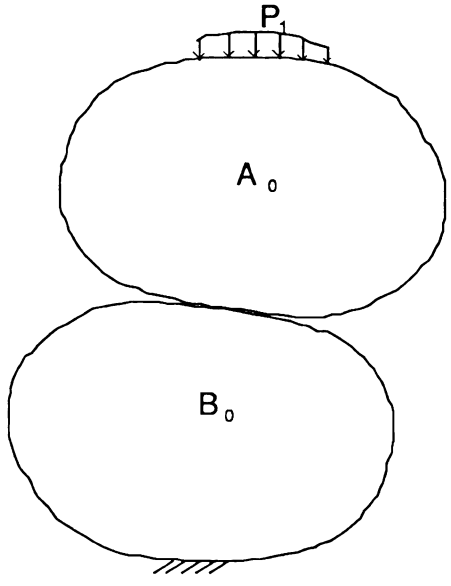

Figure III.5

Contact problem before load step 1 is applied.

The matrices for body A_0 and body B_0 are assembled and related using the initial contact conditions. The load increment P_1 is applied to the system (P_1 is determined by the incremental rules developed), where $P_1 \leq P$. The system of equations is solved for the unknown

quantities giving the equilibrium state for load step 1. The incremental displacements $(\Delta u)_1$ and incremental tractions $(\Delta t)_1$ are now known everywhere on both bodies A and B. We assume for this example that the total externally applied loads have not been applied (P_1<P) and another load step will be applied.

LOAD INCREMENT 2

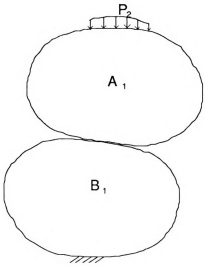

Figure III.6

Contact problem before load step 2 is applied.

The matrices for body A_1 and body B_1 are assembled and related through the contact conditions. The current states A_1 and B_1 are the deformed states at the end of the previous load step. The coordinates of the deformed states are

$$(x_1)_1 = (x_1)_0 + (\Delta u_1)_1$$
$$(x_2)_1 = (x_2)_0 + (\Delta u_2)_1. \qquad \text{(III.4)}$$

The next load increment P_2 is applied to the deformed state at the end of load step 1. Now the system of equations are solved for all unknown quantities, giving the equilibrium state for load step 2. The total displacements and tractions are updated as follows:

$$(t_i)_2 = (t_i)_1 + (\Delta t_i)_2$$
$$(u_i)_2 = (u_i)_1 + (\Delta u_i)_2 . \qquad \text{(III.5)}$$

K^{TH} LOAD INCREMENT

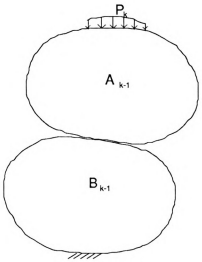

Figure III.7

Contact problem before load step k is applied.

The matrices for body A_{k-1} and body B_{k-1} are assembled and related through the contact conditions. The current states A_{k-1} and B_{k-1} are

the equilibrium states at the end of the previous load step k-1. The coordinates of the deformed states are

$$(x_1)_{k-1} = (x_1)_{k-2} + (\Delta u_1)_{k-1}$$
$$(x_2)_{k-1} = (x_2)_{k-2} + (\Delta u_2)_{k-1}. \qquad \text{(III.6)}$$

The system of equations are solved for the k^{th} time to compute all unknown quantities, and the total quantities are updated once more,

$$(t_i)_k = (t_i)_{k-1} + (\Delta t_i)_k$$
$$(u_i)_k = (u_i)_{k-1} + (\Delta u_i)_k. \qquad \text{(III.7)}$$

This procedure is followed until the m^{th} load step is applied at which time all external loads have been applied to the system. The total displacements and tractions are equal to the sum of all the incremental displacements and tractions,

$$(t_i) = (\Delta t_i)_1 + (\Delta t_i)_2 + \cdots + (\Delta t_i)_m$$

and

$$(u_i) = (\Delta u_i)_1 + (\Delta u_i)_2 + \cdots + (\Delta u_i)_m. \qquad \text{(III.5)}$$

Stresses can now be calculated from the total displacements and tractions.

The incremental algorithm is used to follow the load history as closely as possible. If the increments are sufficiently small, the total quantities are good

approximations to the exact values, but if the analyst chooses too many small increments, the computational requirements are large. An incremental solution can converge to a wrong answer by selecting a load increment that is to large, and this is the case when too many contact conditions are allowed to change in the same load step. Thus, the most important part of the incremental technique becomes the control of how large of a load step to use. The load step should be chosen such that it is as large as possible without sacrificing the accuracy of the analysis. There are two types of approaches to the control of the load step during the incremental process:

1. The load steps can be chosen prior to the analysis using previous knowledge. Then after each load step a convergence check is done. This convergence criterion may be based upon contact conditions remaining constant or equilibrium considerations that sum forces and iterate until the force imbalance is within a tolerance limit. If the convergence test passes, the next load step is applied and then that state is checked for convergence. If the convergence criterion is not satisfied, then the equations are adjusted and solved again. This iterative technique is performed until the convergence criteria is satisfied. Then the next load step is applied and the process repeated until the total load is applied.

2. The load steps can be chosen during the analysis such that within each load step the analysis is numerically linear between discrete points. The total load is applied to the structure, and

based on the changing contact conditions, a scale factor is determined. This scale factor is used to scale back the load to a point where linear equations will simulate the deformation numerically. This would then constitute a load step. The remaining external loads are applied and the process repeated until the total load is applied.

It can be seen that the simple example in Figure III.1 can be simulated using two incremental steps, where within each step the analysis is numerically linear between discrete points. The difference between the two incremental approaches can be demonstrated using the simple example shown in Figure III.1. Using the first approach the initial load step should be as close to P_{gap} as possible. This will keep the number of iterations to a minimum and assure a good solution. If the load step was chosen such that the applied load P was greater than P_{gap} there is a possibility of multiple iterations to achieve the proper convergence conditions. This may also lead to convergence to the wrong answer. If the load is chosen properly ($0 \leq (P - P_{gap}) \leq \varepsilon$, where ε is small) then the approximation will be good. Load steps are then applied until all external loads have been applied and all convergence considerations satisfied. The analysis is very dependent on a preconceived idea of how the system will react under loading. If the analysis is too complex for a good estimation of the load-displacement behavior, then multiple runs will be required to obtain satisfactory results.

The second approach would be to apply the total load P_{total} and, based on a change of contact status at $u=u_{gap}$, calculate a scaling factor. The scaling factor would be equal to P_{gap}/P_{total} and would then be used to scale back the externally

applied loads and all displacement and traction quantities. Load step 1 would then be the applied load P_{gap} that caused the first change of contact status in the contact zone. When the additional load (P_{total} - P_{gap}) was applied, there would be no change of contact status, the scale factor would be equal to 1.0 and the analysis would be completed. Thus the analysis would be completed in two steps without any iterations. This approach is not based on any preconceived idea of the load displacement behavior by the analyst. With this incremental approach the largest possible load step is chosen, while still allowing the analysis to remain numerically linear. Although this is a simple example it shows the capabilities and benefits provided by an automated incremental load step technique. The automated incremental load step procedure is the logic behind the implementation of the analysis program developed in this paper.

III.2 CONTACT WITH AND WITHOUT FRICTION

To simulate bodies in contact, two sets of equations are developed for each of the bodies in contact (see Figure III.8).

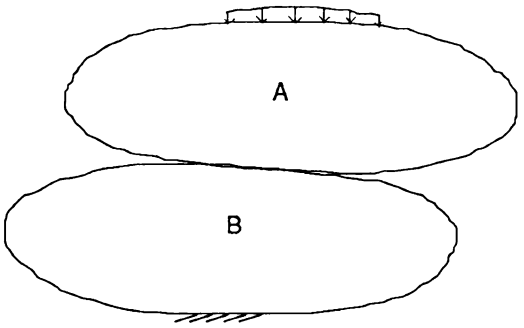

Figure III.8

Two elastic bodies in contact.

The equations are developed for body A and body B and the two sets of equations are then related through the contact region according to the type of contact being simulated. All points in contact are transformed to a local coordinate system, normal and tangent to the boundary, and the contact conditions are imposed. (see Figure III.9)

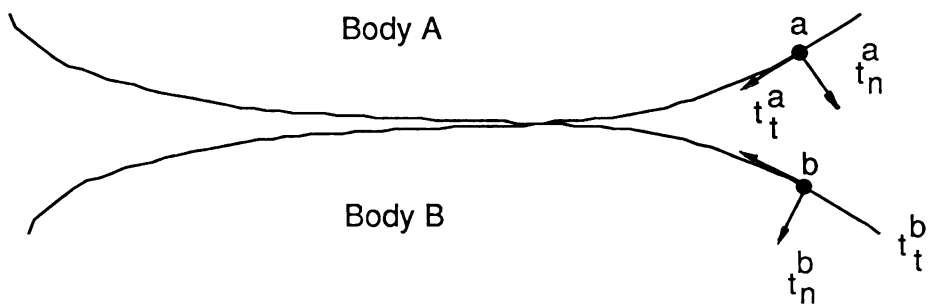

Figure III.9

Enlarged diagram of the contact area.

If the contact problem is considered frictionless, then only normal compressive forces are transmitted from body A to body B. The equations that couple the two sets of integral equations would be:

$$\begin{aligned} -\Delta t_n^a &= \Delta t_n^b, \\ \Delta t_t^a &= 0, \\ \Delta t_t^b &= 0, \\ \Delta u_n^a &= \Delta u_n^b, \end{aligned} \qquad \text{(III.6)}$$

for all nodes in contact. If Coulomb type friction is introduced into the contact region, then normal compressive forces and tangential forces are transferred from body A to body B. For Coulomb type friction the tangential force Δt_t is

related to the normal force Δt_n at each node,

$$\Delta t_t \leq \mu \Delta t_n \tag{III.7}$$

The direction of the tangential force Δt_t is in the opposite direction of impending motion. The contact conditions that couple the two sets of equations, for contact with Coulomb friction, would be

$$\begin{aligned} -\Delta t_n^a &= \Delta t_n^b, \\ -\Delta t_t^a &= \Delta t_t^b, \\ \Delta u_n^a &= \Delta u_n^b, \\ \Delta u_t^a &= \Delta u_t^b, \end{aligned} \tag{III.8}$$

$$\begin{aligned} t_t^a &\leq \mu t_n^a, \\ t_t^b &\leq \mu t_n^b, \end{aligned}$$

for nodal pairs that are in a nonslip state. Although the contact between two bodies introduces nonlinear effects into the system discussed earlier, the problem can be solved using an incremental procedure. The incremental process is a stepwise numerically linear approximation to the nonlinearities that arise. If the assumptions of small displacements and linearly elastic material behavior are made, then an automated incremental procedure can be implemented. The incremental process is used to calculate the contact area for a given load step. Within each load step the problem can be considered numerically linear if the increase in the contact area are small and the contact

conditions remain constant throughout the load step. This is achieved by only allowing the load, during any step, to be large enough to cause the next change of contact status. With the introduction of a load that causes only one change of contact status per load step, the problem is numerically linear within that load step. The three states of contact are as follows:

1. new contact,
2. gapping,
3. change from adhesion to slip.

The first of these conditions to occur controls how large the load increment will be. During the first load step all nodes in contact are assumed to be in an adhesion state and the total external load P is applied. Then for any load step k the total external applied load is

$$P_k = \gamma_k [P - \sum_{i=1}^{k-1} P_i], \qquad \text{(III.9)}$$

where

P_k = applied load after k increments,

P = total external load,

P_i = previous load increment

γ_k = scale factor for the k^{th} increment.

For each load step k, γ_k is calculated to find the next change of contact status. γ_k

is calculated for each change of contact status possible and at each node within the potential contact zone at which that change of contact status could occur. The smallest γ_k calculated will be the scaling factor for the k^{th} load increment. To calculate γ_k for the case of new contact, the relative displacement along the unit direction vector V_i^{ab} must be computed (see Figure III.10).

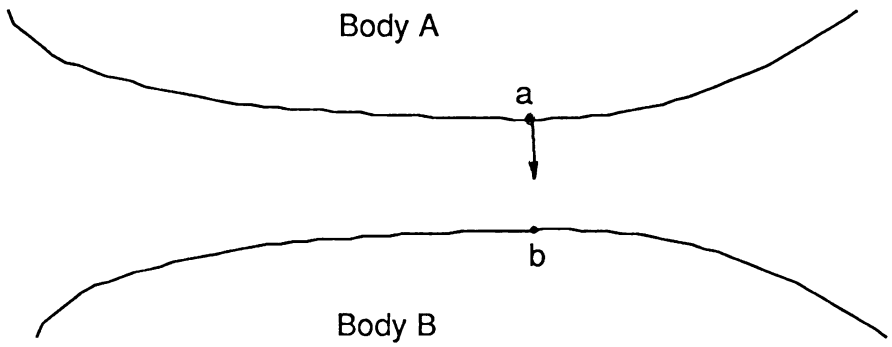

FIGURE III.10

The vector V_i^{ab}.

The displacements along the unit vector V_i^{ab} for nodes a and b are found as follows:

Node a

$$(V_i^{ab})_k \, (u_i^a)_k = (D^a)_k,$$

Node b

$$(V_i^{ab})_k \, (u_i^b)_k = (D^b)_k,$$

where

$(V_i^{ab})_k$ = unit vector from node a to node b for load step k,

$(u_i^a)_k$ = displacement vector for node a for load step k,

$(u_i^b)_k$ = displacement vector for node b for load step k,

$(D^a)_k$ = the magnitude of the displacement vector $(u_i^a)_k$ along the vector $(V_i^{ab})_k$ for load step k,

$(D^b)_k$ = the magnitude of the displacement vector $(u_i^b)_k$ along the vector $(V_i^{ab})_k$ for load step k.

Since the displacements of node a and node b along the vector V_i^{ab} are known, the relative displacement $(D^{ab})_k$ can be calculated,

$$(D^{ab})_k = (D^a)_k - (D^b)_k. \qquad \text{(III.10)}$$

The scaling factor γ_κ, for the change of contact status to new contact, during the k^{th} load increment, can be calculated as follows:

$$\gamma_\kappa = (G^{ab})_k/(D^{ab})_k, \qquad \text{(III.11)}$$

where

$(D^{ab})_k$ = the relative displacement between node a and node b for load step k,

$(G_{ab})_k$ = the nodal gap between nodes a and b at the end of load step k-1.

The contact conditions for this set of nodes now becomes

$$-\Delta t_n^a = \Delta t_n^b$$
$$\Delta u_n^a = \Delta u_n^b,$$

for frictionless contact and

$$-\Delta t_n^a = \Delta t_n^b,$$
$$-\Delta t_t^a = \Delta t_t^b,$$
$$\Delta u_n^a = \Delta u_n^b$$
$$\Delta u_t^a = \Delta u_t^b,$$

for contact with friction and in a non-slip state.

To calculate γ_k for the case of a nodal pair already in contact pulling apart and gapping, the load history of the normal force between the contact nodes must be followed. To be in contact there must be a compressive normal force between the nodes of the nodal pair. If the force between bodies goes from compressive to tensile, then the two nodes will tend to gap and there is a point in this process where the normal force is zero. The point during the application of the load where the normal force is zero is the point where the nodal pair will begin to pull apart or gap. The scale factor γ_k is calculated such that it will scale the applied load to the point where the normal force between the contacting nodal pairs is zero. This is accomplished by first calculating the next tangential force $(\Delta t_t)_k$ that occurs when the remaining load

$$P - \sum_{i=1}^{k-1} P_i$$

is applied to the equilibrium state of the k-1 load step. The value $(t_n^a)_{k-1}$ represents the total compressive force between nodal pairs in contact. The value $(\Delta t_n^a)_{k'}$ if negative, represents a tensile force between nodal pairs which indicates the nodal pairs will gap. The scale factor γ_k should be calculated such that the force between nodal pairs is zero. At this point the condition of nodal contact is removed. The point where the nodal force between the nodes is zero can be calculated as follows:

$$(t_n^a)_{k-1} + (\Delta t_n^a)_k = 0 \qquad \text{(III.11)}$$

$$(\Delta t_n^a)_k = -(t_n^a)_{k-1}$$

$$\gamma_k(\Delta t_n^a)_{k'} = -(t_n^a)_{k-1}$$

$$\gamma_k = -(t_n^a)_{k-1}/(\Delta t_n^a)_{k'} \qquad \text{(III.12)}$$

which will be a postive number. The contact conditions for this set of nodal pairs becomes

$$\Delta t_t^a = \Delta t_t^b = 0$$

$$\Delta t_n^a = \Delta t_n^b = 0. \qquad \text{(III.13)}$$

The change of contact status from adhesion to slip will occur when the total tangential force t_t becomes greater than the maximum allowable shear force t_t^{max}, where

$$t_t^{max} = \mu \Delta t_n. \qquad \text{(III.14)}$$

After load step k-1 has been applied and the contact is in a non-slip state the relationship between the tangential force t_t^a and the normal force t_n^a is

$$(\Delta t_t^a)_{k-1} \leq \mu(\Delta t_n^a)_{k-1}. \tag{III.15}$$

If during the k^{th} load step a nodal pair is to slip then the following must be true,

$$(\Delta t_t^a)_k > \mu(\Delta t_n^a)_k$$

or (III.16)

$$\gamma_k(\Delta t_t^a)_{k'} > \mu\gamma_k(\Delta t_n^a)_{k'}.$$

The scale factor γ_k can be calculated to find the percentage of the applied load at which point

$$(t_t^a)_k = \mu(t_n^a)_k. \tag{III.17}$$

Equation (III.17) can be rewritten in the following form

$$(t_t^a)_{k-1} + \gamma_k(\Delta t_t^a)_{k'} = \mu[(t_n^a)_{k-1} + \gamma_k(\Delta t_n^a)_{k'}]. \tag{III.18}$$

Equation (III.18) may now be solved for the scaling factor γ_k giving

$$\gamma_k = [(t_n^a)_{k-1} - (t_t^a)_{k-1}]/[(\Delta t_t^a)_{k'} - \mu(\Delta t_n^a)_k]. \tag{III.19}$$

The new contact conditions for the nodal pair are

$$-\Delta t_n^a = \Delta t_n^b,$$
$$\Delta u_n^a = \Delta u_n^b,$$

$$\Delta t_t^a = \mu \Delta t_n^a$$

$$\Delta t_t^b = \mu \Delta t_n^b,$$

for contact with friction.

When a nodal pair changes state from adhesion to slip, the two nodes begin to move apart relative to each other in a tangential direction, the basic assumption of small displacement is violated. The violation is because the arc length between discrete nodal points must change in order to accommodate the slip condition experienced. The boundary of each body is divided into a finite number of discrete points, and in the potential contact region of both bodies the pair of contact elements that are opposite and expected to come into contact should have the same arc length (see Figure III.11).

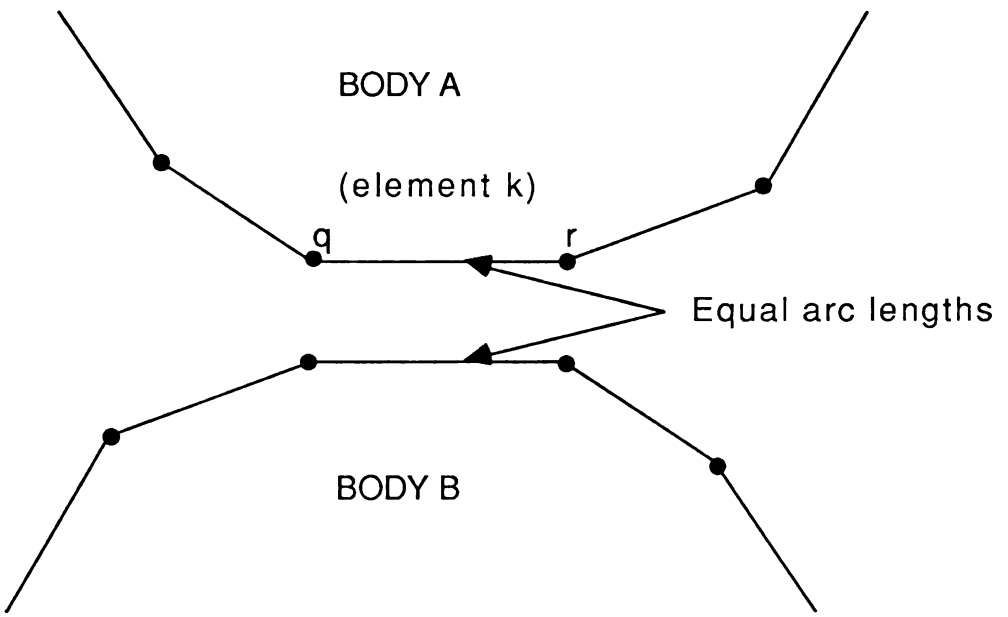

Figure III.11

The boundary divided into discrete elements.

It is then assumed that due to small displacement theory, the arc lengths of opposite elements modeled with equal arc lengths before deformation, will have approximately the same arc lengths after deformation due to loading. This will allow successive nodal pairs in later load steps to come into contact. If node q on one side of element k, is allowed to slide, while node r is in the adhesion state with its nodal pair, then the arc length of element k must expand or contract thus violating the assumption of small displacements that allow successive nodal pairs to come into contact. If all nodal pairs begin to slide then a rigid body motion occurs and the problem is no longer static.

III.3 THE BOUNDARY ELEMENT EQUATIONS APPLIED TO PROBLEMS INVOLVING CONTACT

The implementation of the Boundary Integral Equations to solve problems involving bodies in contact is a straightforward extension of the equations developed in Chapter II. A set of Boundary Integral Equations are developed for each of the bodies in contact for every load increment

Body A

$$\alpha'_{ij}(\underline{x})\Delta u_j(\underline{x}) \; - \; \oint_A (uc)_{ij}(\underline{x},\zeta)\Delta u_j(\zeta)ds \; = \; \int_A (uR)_{ij}(\underline{x},\zeta)\Delta t_j(\zeta)ds,$$

Body B (III.20)

$$\alpha'_{ij}(\underline{x})\Delta u_j(\underline{x}) \; - \; \oint_B (uc)_{ij}(\underline{x},\zeta)\Delta u_j(\zeta)ds \; = \; \int_B (uR)_{ij}(\underline{x},\zeta)\, t_j(\zeta)ds,$$

and then related through the contact region.

Now the Boundary Integral Equations must be written in a form to be used in an incremental formulation. The incremental form of the Boundary Integral Equation is as follows:

$$\alpha'_{ij}(x)\Delta u_j(x) - \int_B (uc)_{ij}(x,\zeta)\Delta u_j(\zeta)ds = \int_B (uR)_{ij}(x,\zeta)\Delta t_j(\zeta)ds \qquad (III.21)$$

Then the unknown tractions Δt_i and displacements Δu_i are determined for each load step. The total tractions and displacements are equal to the sum of all the incremental tractions and displacements,

$$t_i = \sum_{k=1}^{m} (\Delta t_i)_k$$

and (III.22)

$$u_i = \sum_{k=1}^{m} (\Delta u_i)_k.$$

The incremental procedure developed earlier in this chapter is based on introducing only one change of status in each increment. Then for each load step the simulation remains numerically linear between discrete points and the incremental Boundary Integral Equations (III.21) can be used. The algorithm for calculating the scaling factor γ_k for the k^{th} load step is used to find the exact load level at which the the next change in contact status will occur. The next load step is applied and again the incremental Boundary Integral Equations (III.21) are used to solve for the unknown displacements and tractions. This procedure is followed until the m^{th} load step is applied and $\gamma_m = 1.0$. This means that all externally applied loads have been applied and the analysis is completed.

Since Somigliana's identity can only be solved for some geometries with simple

traction and displacement functions, as stated in Chapter II, the boundary is broken into N segments. Then over each segment an approximate function to the actual variation of the displacements and tractions is chosen. The integral over the entire boundary then becomes a summation of N integrals over each individual segment. The numerical form of the boundary equation for an incremental procedure then becomes,

$$\alpha'_{ij}(x^n)\Delta u_j(x^n) + \sum_{m=1}^{N}\int_m (uc)_{ij}(x^n,\zeta)\Delta u_j(\zeta)ds = \sum_{m=1}^{N}\int_m (uR)_{ij}(x^n,\zeta)\Delta t_j(\zeta)ds. \qquad \text{(III.23)}$$

where Equation (III.23) is developed for each body. The numerical procedure developed here uses a linear variation for the displacement function and a constant variation for the traction function over each segment. To simplify the integration over each segment further, shape functions are used to approximate the variation of the displacements over each segment (boundary element),

$$\begin{aligned} u_j &= u_j^{m-1}N_1(\xi) + u_j^{m}N_2(\xi), \\ t_j &= t_j^{m}, \\ N_1(\xi) &= .5(1-\xi), \\ N_2(\xi) &= .5(1+\xi), \\ ds &= .5(s_m - s_{m-1})d\xi = .5\Delta s_m d\xi, \end{aligned} \qquad \text{(III.24)}$$

where

u_j^{m-1} = the displacement at the beginning of element n,

u_j^{m} = the displacement at the end of element n,

ξ = local coordinate that varies from -1 to 1,

N_i = shape functions,

Δs_m = length of element m.

Substituting Equations (III.24) into Equation (III.23) gives,

$$2\alpha'_{ij}(x^n)\Delta u_j^n + \sum_{m=1}^{N}\Delta s_m\left[\Delta u_j^{m-1}\int_m (uc)_{ij}(x^n,\xi)N_1(\xi)d\xi + \Delta u_j^m\int_m (uc)_{ij}(x^n,\xi)N_2(\xi)d\xi\right] = \sum_{m=1}^{N}\Delta s_m\Delta t_j^m\int_m (uR)_{ij}(x^n,\xi)d\xi \qquad \text{(III.25)}$$

Equation (III.25) is developed for each body and the supplemental contact equations are used to relate the two systems of equations. This is the same equation developed in Chapter II, but now it is applied to each of the two bodies the and two sets of equations are coupled through the contact conditions.

For a plane problem using a Boundary Integral formulation, the number of degrees of freedom per node is four. There are two tractions and two displacement terms for each node. For every node except the nodes in contact, two degrees of freedom are known, thus giving two unknowns and two equations per node. In the contact region the displacements and tractions are expressed in terms of a local coordinate system, which is normal and tangent to the boundary. For contact without friction, the number of unknowns per contact nodal pair is six. For contact with friction, the number of unknowns per contact nodal pair is eight, while Somigliana's Identity provides only four equations, two for each body. This means that for the case of contact with friction there are four more unknown terms per nodal pair in the contact region. Therefore the equations generated using Somigliana's identity must be supplemented in order to have the same number of equations as unknowns. The number of unknown tractions and displacements for the two bodies in contact, body A and body B, would be,

unknowns = 2(non-contact nodes on body A and B) + 4(contact nodal pairs).

The number of equations that can be generated are,

equations = 2•[(nodes on A) + (nodes on B)],

for contact with friction. To supplement these equations and relate the equations of body A to the equations of body B we use the contact conditions,

$$-\Delta t_n^a = \Delta t_n^b,$$
$$-\Delta t_t^a = \Delta t_t^b,$$
$$\Delta u_t^a = \Delta u_t^b,$$

and (III.26)

$$\Delta u_n^a = \Delta u_n^b,$$

for the case of contact with friction. These contact conditions supplement four equations for every nodal pair in contact. Thus there are the same number of equations as unknowns, and the equations of body A are related to the equations of body B through the supplemental contact equations. This set of equations can now be solved for all unknown displacements and tractions.

III.4 COMPUTER IMPLEMENTATION

The flow of the incremental contact program is similar to the program described in Chapter II. First the coefficient matrices [uc] and [uR] are formed for each

body A and B, from the boundary coordinates and material information. Each set of equations can be expressed as follows:

Body A

$$[uc]_A G_A \{\Delta u\}_A = [uR]_A \{\Delta F\}_A,$$

Body B (III.27)

$$[uc]_A G_B \{\Delta u\}_B = [uR]_B \{\Delta F\}_B.$$

This set of equations can be written in the following matrix form:

$$\begin{bmatrix} [uc]_A & 0 \\ 0 & [uc]_B \end{bmatrix} \begin{bmatrix} G_A \Delta u_A \\ G_B \Delta u_B \end{bmatrix} = \begin{bmatrix} [uR]_A & 0 \\ 0 & [uR]_B \end{bmatrix} \begin{bmatrix} \Delta F_A \\ \Delta F_B \end{bmatrix}.$$

Each system of equations relates nodal displacements to resultant segment forces. To create a well-posed problem relating nodal displacements to nodal forces, a transformation is required. If we let

$$\Delta \mathbf{F}_i^m = .5\,(\Delta F_i^m + \Delta F_i^{m+1}), \qquad \text{(III.28)}$$

then a transformation matrix can be written such that

$$\{\Delta \mathbf{F}\} = [T]\{\Delta F\}, \qquad \text{(III.29)}$$

where

$$[T] = .5\begin{bmatrix} I & I & O & O & \cdot & O \\ O & I & I & O & \cdot & O \\ O & O & I & I & \cdot & O \\ O & O & O & I & \cdot & O \\ \cdot & \cdot & \cdot & \cdot & \cdot & \cdot \\ I & O & O & O & \cdot & I \end{bmatrix},$$

and I is a 2x2 identity matrix

$$I = \begin{bmatrix} 1 & 0 \\ 0 & 1 \end{bmatrix}.$$

Equation (III.29) can now be rearranged by multiplying both sides by $[T]^{-1}$ giving the following:

$$[T]^{-1}\{\Delta F\} = \{\Delta F\}$$

This transformation is performed on both systems of equations.

Body A

$$[uc]_A G_A \{\Delta u\}_A = [uR]_A [T]_A^{-1} \{\Delta F\}_A,$$

Body B

$$[uc]_B G_A \{\Delta u\}_B = [uR]_B [T]_B^{-1} \{\Delta F\}_B,$$

where

$$[T]^{-1} = \begin{bmatrix} I & -I & I & -I & \cdot & I \\ I & I & -I & I & \cdot & -I \\ -I & I & I & -I & \cdot & I \\ I & -I & I & I & \cdot & -I \\ \cdot & \cdot & \cdot & \cdot & \cdot & \cdot \\ -I & I & -I & I & \cdot & I \end{bmatrix},$$

provided that the number of nodes is odd. The next step in the computer program is to post multiply the matrix [uR] by the inverse of the transformation matrix. Now the system of equations is as follows:

$$\begin{bmatrix} [uc]_A & 0 \\ 0 & [uc]_B \end{bmatrix} \begin{bmatrix} G_A \Delta u_A \\ G_B \Delta u_B \end{bmatrix} = \begin{bmatrix} [M]_A & 0 \\ 0 & [M]_B \end{bmatrix} \begin{bmatrix} \Delta F_A \\ \Delta F_B \end{bmatrix}, \tag{III.30}$$

where

$$[M] = [uR][T]^{-1}$$

This equation relates the displacements and tractions at any point P with all other tractions and displacements everywhere on the boundary. This is true for both sets of equations involving body A and body B. To enforce equilibrium on both systems of equations, a supplemental set of equations are augmented that will insure equilibrium. The three supplemental equations for each body are,

1. The summation of the forces in the X direction;

$$\sum_{i=1}^{N} \Delta F_1^i = 0,$$

2. The summation of the forces in the X_2 direction;

$$\sum_{i=1}^{N} \Delta F_2^i = 0,$$

3. The summation of the moment about node 1;

$$\sum_{i=1}^{N} (X_1 \Delta F_2^i - X_2 \Delta F_1^i) = 0.$$

In matrix form this can be expressed as,

$$[Q]\{\Delta F\} = \{0\},$$

where

$$[Q] = \begin{bmatrix} 1 & 0 & 1 & 0 & \cdots & 1 & 0 \\ 0 & 1 & 0 & 1 & \cdots & 0 & 1 \\ 0 & 0 & x_2^1 - x_2^2 & x_1^2 - x_1^1 & \cdots & x_2^1 - x_2^N & x_1^N - x_1^1 \end{bmatrix}.$$

The system of equations now becomes,

$$\begin{bmatrix} 0 & 0 & & \\ -[Q]_A^T & [uc]_A & 0 & \\ & & [uc]_B & -[Q]_B^T \\ 0 & & 0 & 0 \end{bmatrix} \begin{bmatrix} \lambda_A \\ \{u\}_A \\ \{u\}_B \\ \lambda_B \end{bmatrix} = \begin{bmatrix} [Q]_A & & \\ [M]_A & 0 & \\ 0 & [M]_B & \\ & [Q]_B & \end{bmatrix} \begin{bmatrix} \\ \{F\}_A \\ \{F\}_B \\ \end{bmatrix}$$

(III.31)

The equations for body A and body B are unrelated at this point in the program. Therefore this system of equations needs to be coupled through the contact region as described earlier in this chapter. In order to use the contact conditions to couple the system of equations, the nodal pairs coming into contact must be transformed into a local coordinate system. The local coordinate system is defined by the mean normal between the nodes in contact on body A and body B. The calculation of this mean normal is described in Appendix C. A transformation matrix [L] is used to transform the coefficients of the nodes in contact for both bodies to a local coordinate system, normal and tangent to the boundary. The transformation matrix [L] is of the following form:

$$[L] = \begin{bmatrix} \cos\theta_m & \sin\theta_m \\ -\sin\theta_m & \cos\theta_m \end{bmatrix}.$$

After the transformation is made the system of Equations (III.31) become:

(III.32)

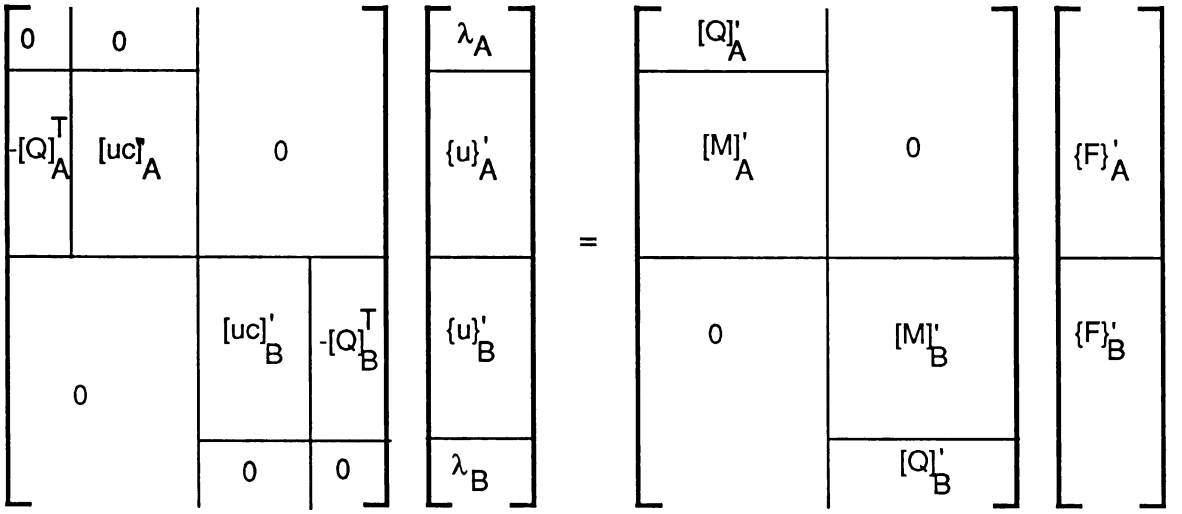

Equation (III.32) has both unknown displacements and unknown tractions, so to set up a system of equations that can be solved for the unknowns, equation (III.32) must be rearranged. Also, Equation (III.32) still has two sets of uncoupled equations, which need to be modified to incorporate the contact conditions. The contact conditions that relate the two sets of equations are of the form

$$u_n^a = u_n^b.$$

This condition can be inforced by moving the coefficients that multiply u_n^b in the left hand side matrix so that they multiply u_n^a. The column that contained the coefficients is then removed. A similar process is preformed to enforce the other contact conditions. All unknown forces and the coefficients that multiply them are moved from the right hand side of equation (III.32) to the left hand side of

equation (III.32). The corresponding known displacements and the coefficients that multiply them are moved to the right hand side of equation (III.32). Once all unknown quantities are in the left hand side vector and all known quantities are in the right hand side vector, the two matrices on the right hand side are multiplied together to produce a column matrix of real numbers. The system of equations now looks like

$$[A]\{x\} = \{B\}, \qquad \text{(III.33)}$$

where

- $\{x\}$ = contains unknown tractions, displacements and six terms related to the equilibrium equations,
- $[A]$ = the coefficients of [uc] and modified [uR] that multiply the unknown matrix $\{x\}$,
- $\{B\}$ = the resultant matrix of matrices that were multiplied together.

At this point the nodal gap between perspective nodal pairs is calculated. The gap is calculated as the distance between potential nodal pairs along a vector between nodal pairs in the direction from body A to body B. The set of nodal gaps are stored for later use in determining the scaling factor for the current load step.

Equation (III.33) can now be solved for the column matrix $\{x\}$ of unknown quantities. When the results for $\{x\}$ are obtained, a complete set of incremental boundary information is known. The scaling factor γ_κ can now be calculated using the procedure described earlier in this chapter. The purpose of the scaling

factor is to find the percentage of the applied load step that will cause the next change in the contact status. Thus providing that the equations will remain numerically linear throughout the load step. The total displacements and tractions are updated by adding the incremental quantities to the total quantities from the previous load step. If $\gamma_\kappa = 1.0$ then the total external load has been applied and the analysis is complete.

$$(t_n)_k = (t_n)_{k-1} + \Delta(t_n)_k$$
$$(t_t)_k = (t_t)_{k-1} + \Delta(t_t)_k$$
$$(u_n)_k = (u_n)_{k-1} + \Delta(u_n)_k$$
$$(u_t)_k = (u_t)_{k-1} + \Delta(u_t)_k \qquad \text{(III.34)}$$

If $\gamma_\kappa < 1.0$ then the coordinates must be updated to reflect the deformation from the last load step and the complete process is repeated. Once the total displacements and tractions have been updated for the last time, to give the final quantities on the boundary, the displacements and stresses anywhere in the domain R of each body can be calculated from the numerical form of Equations (II.11) and (II.13) for each body A and B.

CHAPTER IV

RESULTS

IV.1 EXAMPLES

The procedures developed in the previous chapters will be applied to example problems with analytical solutions, so that a comparison can be established. The first example is the solution of two parallel cylinders in contact. Both cylinders have a radius of 1.0 and are infinite in length (see figure IV.1).

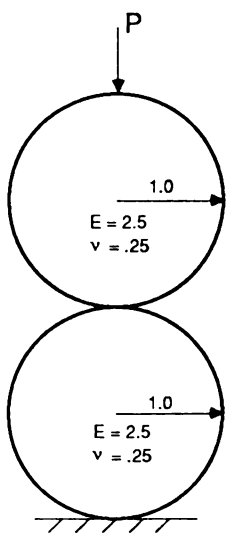

Figure IV.1

Two parallel cylinders, with radii of 1.0, in contact.

The examples problems solved for were made of the same material and had the following material properties

$E = 2.5$

$\nu = .25$

The applied load versus contact area is compared to the analytical solution found in the Handbook of Stress and Strength [2]. Multiple runs were made with different degrees of discretization to test the effect of mesh density on the a numerical results. The boundary of the two cylinders is all that needs to be modeled, when using a boundary integral formulation, as opposed to a finite element solution which would discretize the total domain. It can be seen from this simple example that when the boundary integral method is used, the data preparation is decreased dramatically.

The second example is for the solution of a cylinder on an elastic foundation. The radius of the cylinder is 1.0, and the width of the foundation is 4.0 (see figure IV.2).

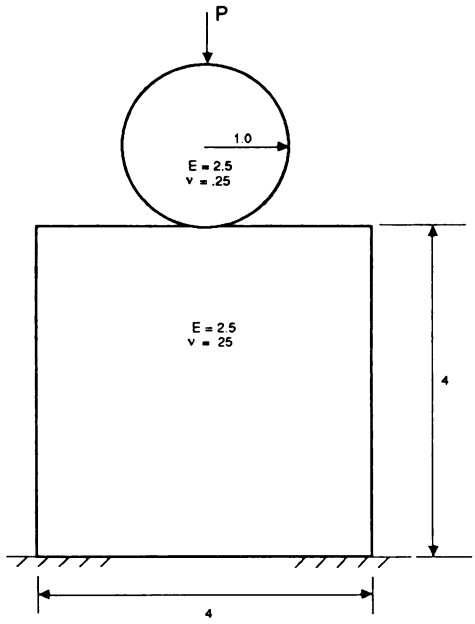

Figure IV.2

A cylinder of radius 1.0, in contact with an elastic foundation.

Both bodies where made of the same material having the following properties

$$E = 2.5$$

$$\nu = .25$$

The load versus the contact area is compared to the analytical solution found in the Handbook of Stress and Strength [2]. Again multiple runs are made to see the accuracy at various discretization levels.

As seen in Fiqure IV.3 the pressure distribution is parabolic and constant along the length of the cylinders. Although Figure IV.3 is for two cylinders in contact, the same type of pressure distribution occurs for contact involving a cylinder on an elastic foundation. Both examples can be simulated using a plane model and assuming a unit thickness. The applied load P verses the contact area b is used as the comparison between the analytical results and the numerical results from the development program. The analytical results as presented in the Handbook of stress and strength [2] for two cylinders in contact is

$$b = 1.13\ [P\Delta(a(1/R_1 + 1/R_2))]^{1/2}$$

and for a cylinder on an elastic foundation the equation is

$$b = 1.13[PR\Delta/a]^{1/2}.$$

For both examples the model is for a unit thickness

$$a = 1.0$$

and the radii are

$$R = R_1 = R_2 = 1.0$$

The variable Δ is evaluated using the following formulation

$$\Delta = (1-\nu_1^2)/E_1 + (1-\nu_2^2)/E_2$$

where

$$\nu_1 = \nu_2 = .25$$

and

$$E_1 = E_2 = 2.5.$$

This gives a value of

$$\Delta = .75$$

for both contact problems. The final equations for the contact area b versus the applied load are

$$b = .69198085P^{1/2}$$

for contact between two cylinders and

$$b = .9786087P^{1/2}$$

for the contact of a cylinder on an elastic foundation. For a definition of a, b and R see Figures IV.3 and IV.4.

Table IV.1 and Table IV.2 contain a summary of the discription for both examples. Table IV.3 and Table IV.4 contain the analytical and numerical results for the contact area b verses the applied load P for example 1 and example 2. Figures IV.5 through IV.8 show all 4 models for example 1. Figures IV.9 through IV.12 show all 4 models for example 2. The numerical results are also plotted against the analytical curve for example 1 in Figure IV.13 and for example 2 in Figure IV.14.

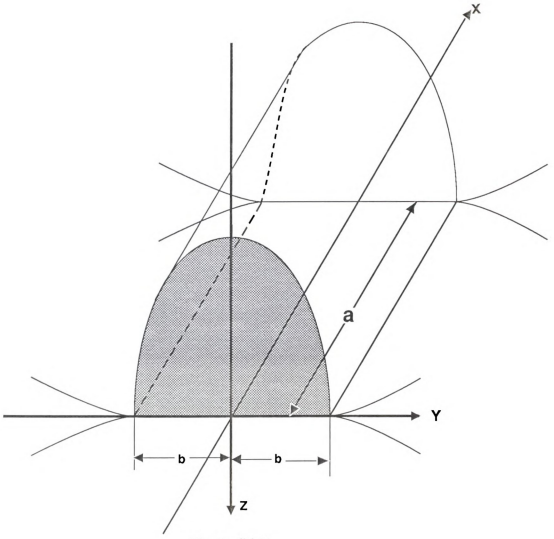

Figure IV.3

Pressure distribution along the length of 2 cylinders in contact.

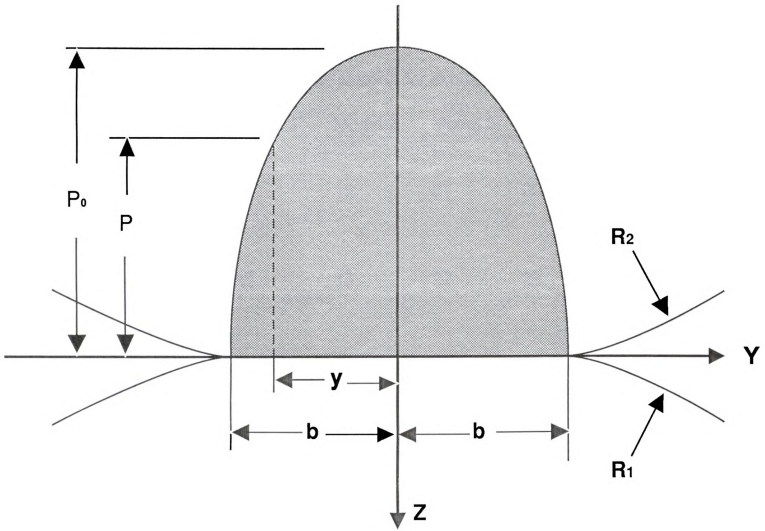

Figure IV.4

Pressure distribution of two cylinders in contact shown in 2 dimensions.

Table IV.2

Model description for example 2.

	Model 1	Model 2	Model 3	Model 4
Number of elements body 1	19	21	31	35
Number of elements body 2	13	15	25	29
Number of contact pairs	7	7	9	11

Table IV.3
Contact area versus applied load for discrete nodal points of example 1.

Contact Area b	Applied Load (Analytical) P	Applied Load (Model 1) P	Applied Load (Model 2) P	Applied Load (Model 3) P	Applied Load (Model 4) P
.02094	.00091	.00054	.00056	.00044	.00044
.04188	.00366			.00262	.00262
.06282	.00824			.00714	.00718
.08376	.01465	.00648	.00674	.00782	.00782
.1047	.02289			.02053	.02063
.12564	.03296			.02822	.02932
.14658	.04487	.05398	.04504	.04500	.04501

Table IV.4

Contact area versus applied load for discrete nodal points of example 2.

Contact Area b	Applied Load (Analytical) P	Applied Load (Model 1) P	Applied Load (Model 2) P	Applied Load (Model 3) P	Applied Load (Model 4) P
.02094	.00045	.00028	.00022	.00022	.00022
.04188	.00183			.00130	.00130
.06282	.00412			.00326	.00332
.08376	.00732	.00410	.00424	.00602	.00615
.10470	.01144			.00858	.00908
.12564	.01648			.01362	.01610
.14658	.02243	.02112	.02006	.01956	.01966

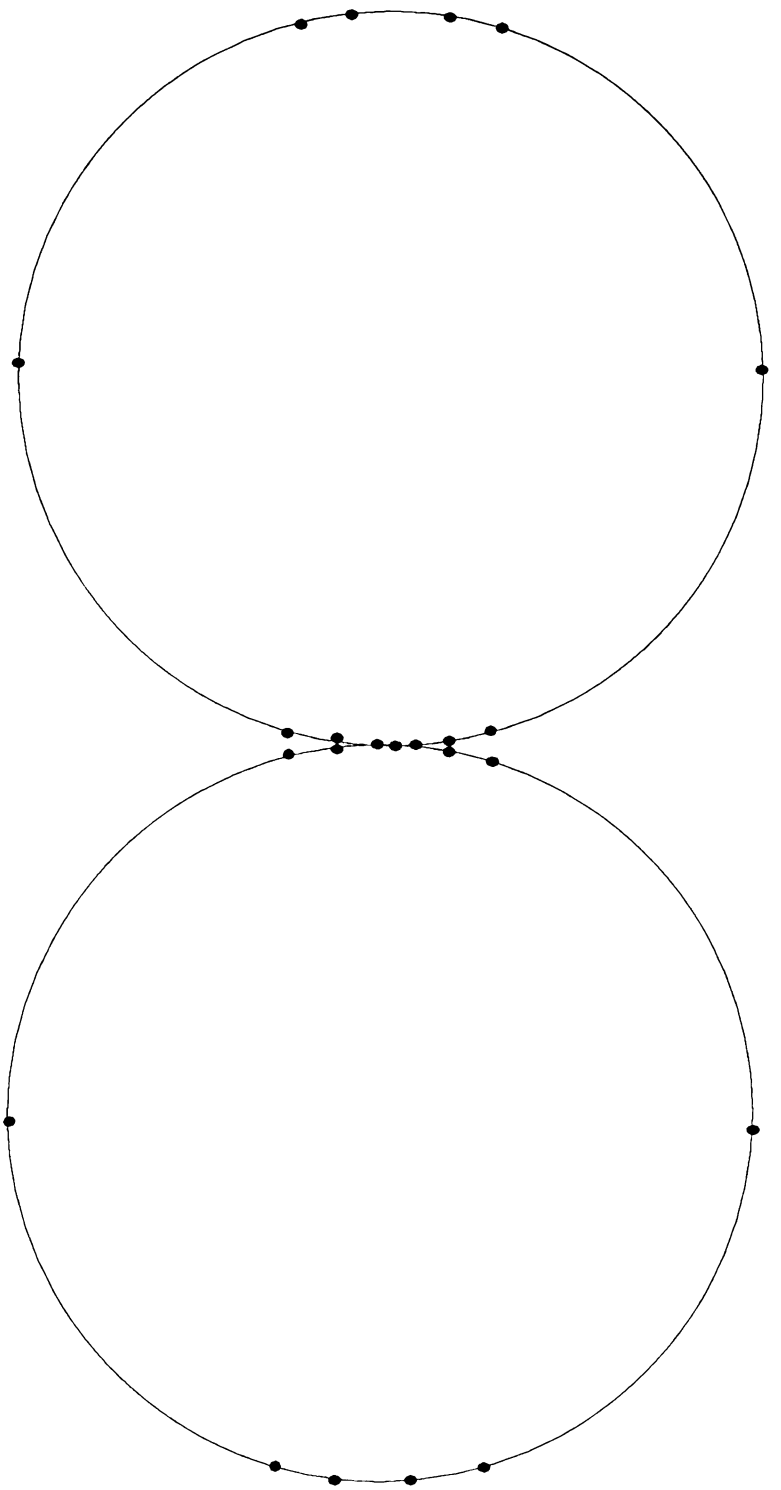

Figure IV.5
Model 1 example 1 (not to scale).

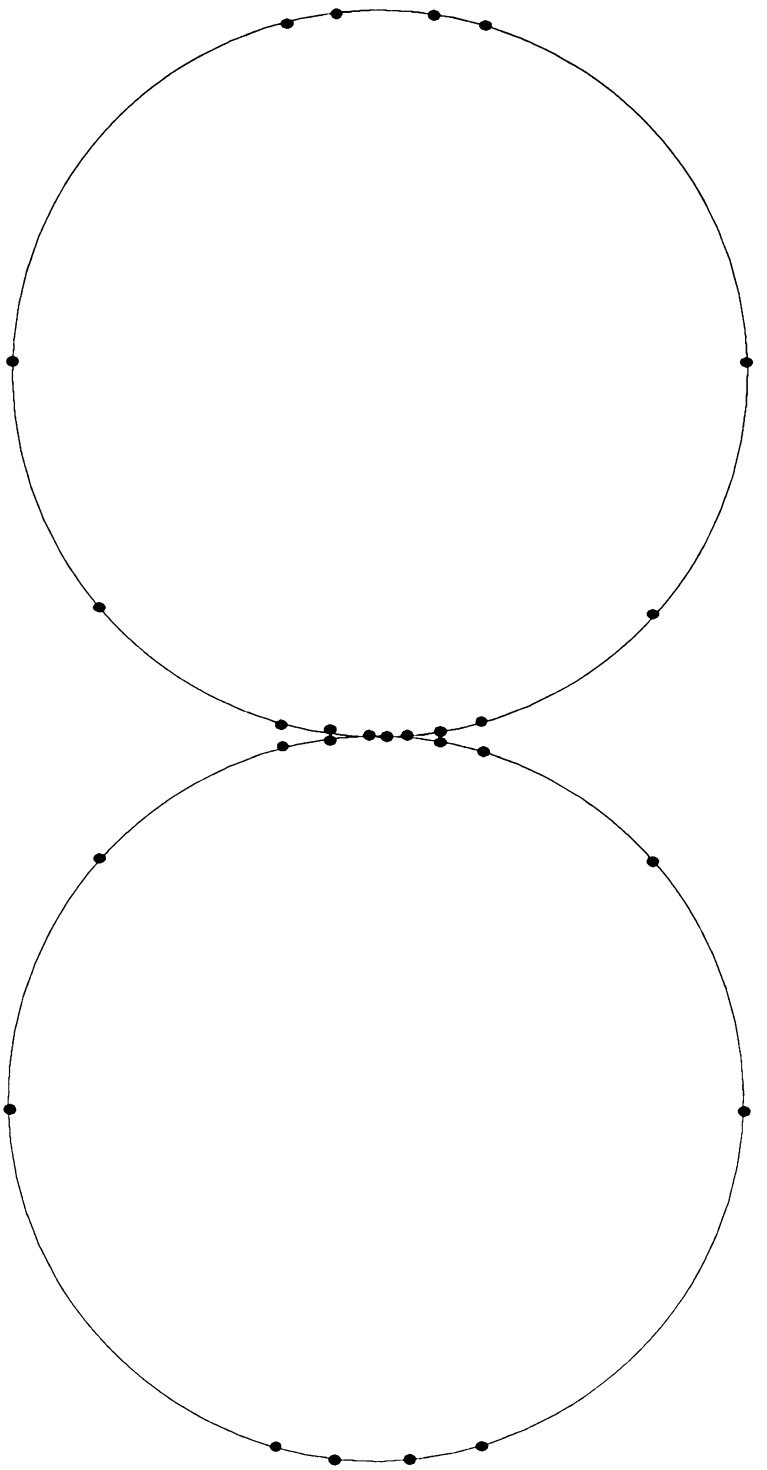

Figure IV.6
Model 2 example 1 (not to scale).

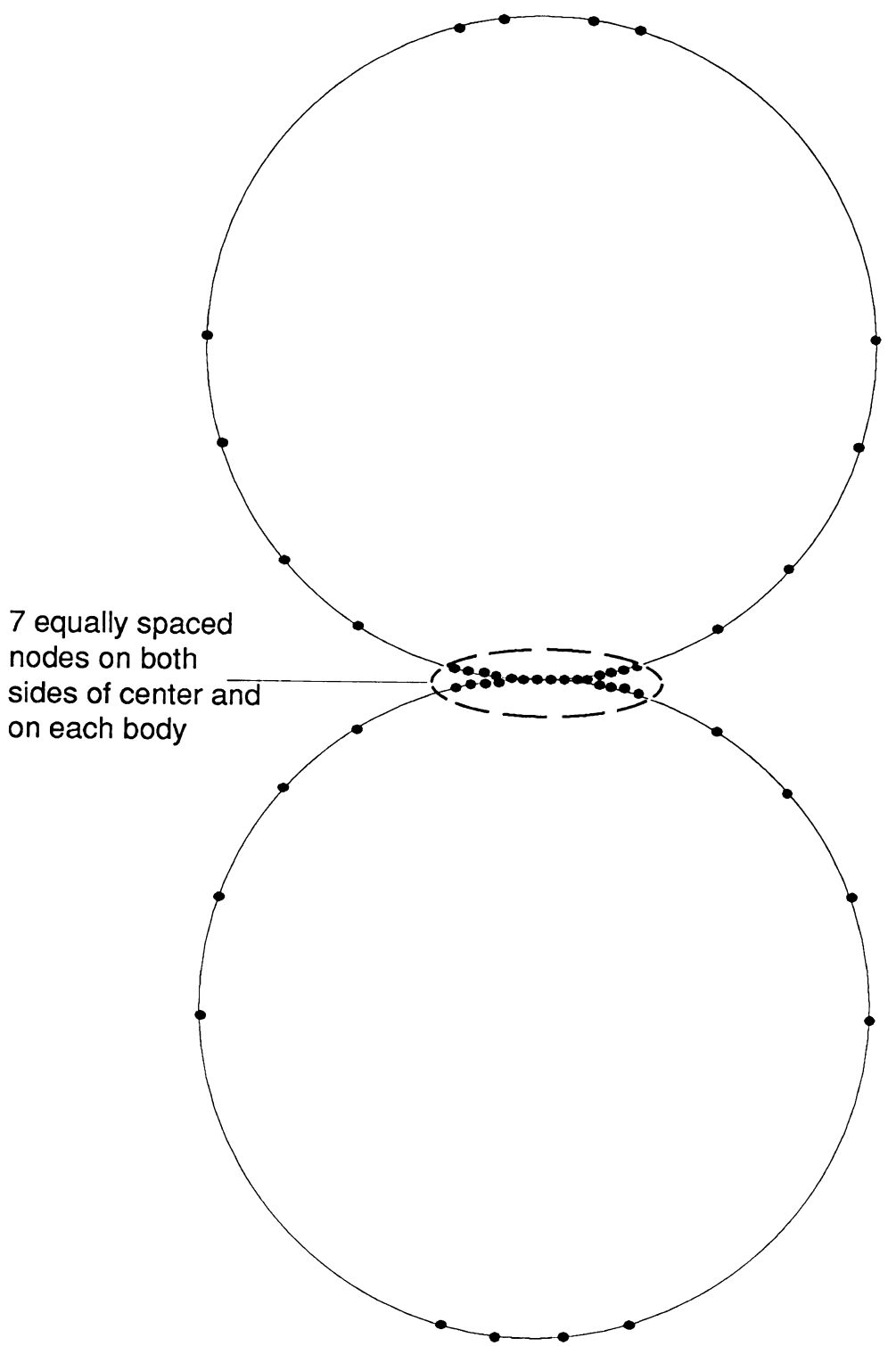

Figure IV.7
Model 3 example 1 (not to scale).

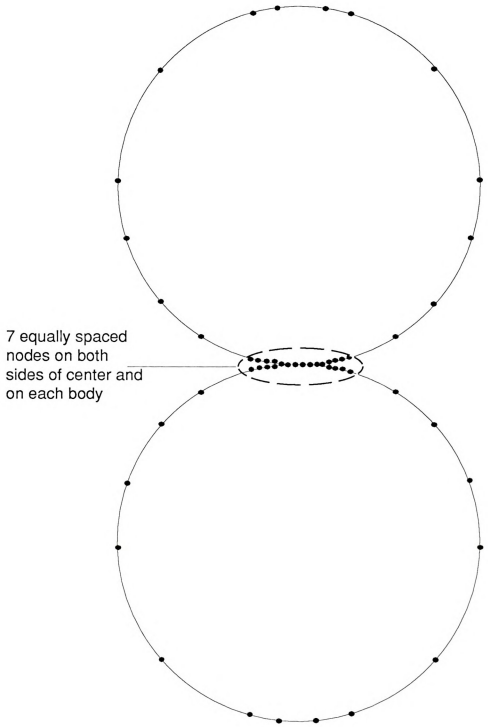

Figure IV.8
Model 4 example 1 (not to scale).

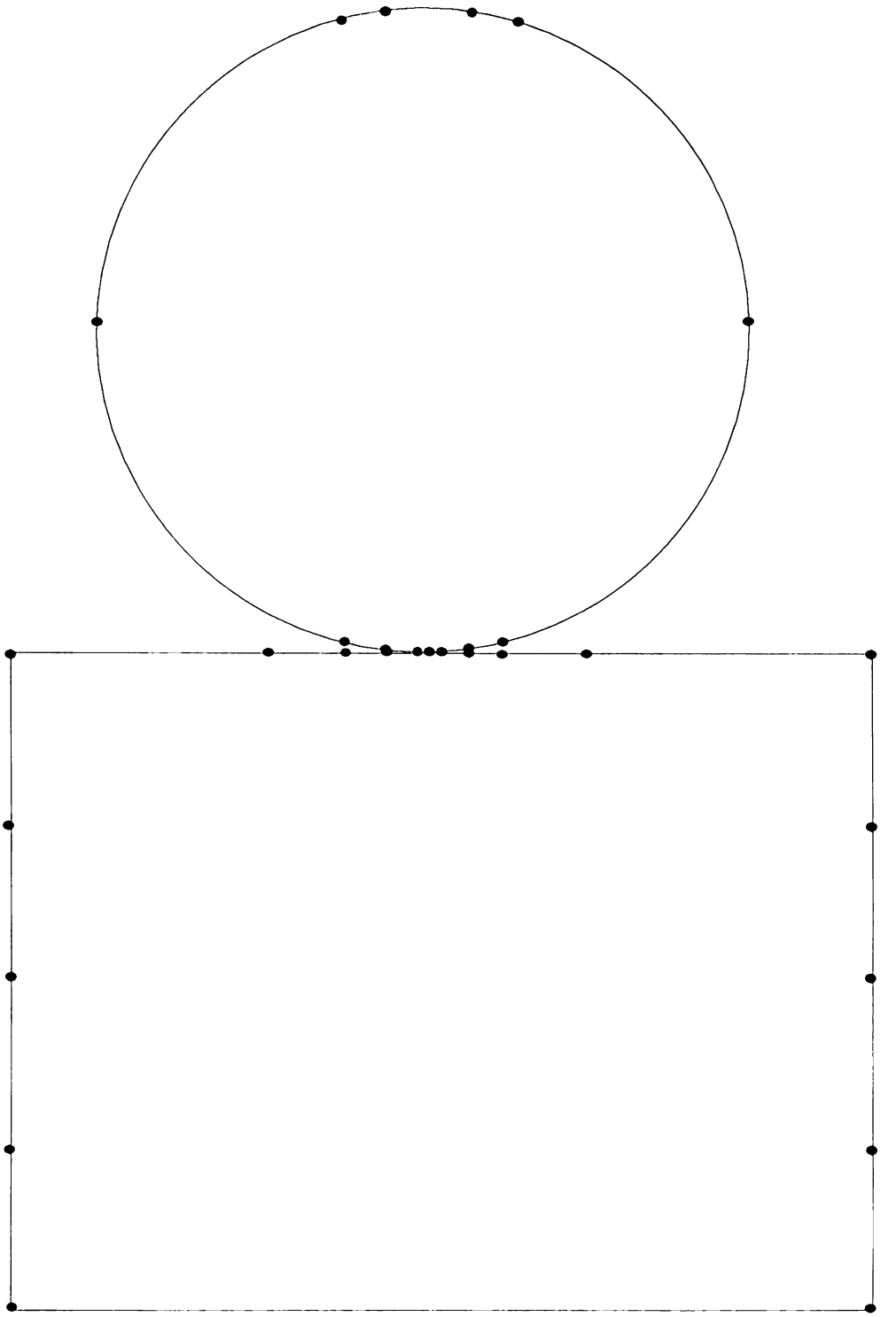

Figure IV.9
Model 1 example 2 (not to scale).

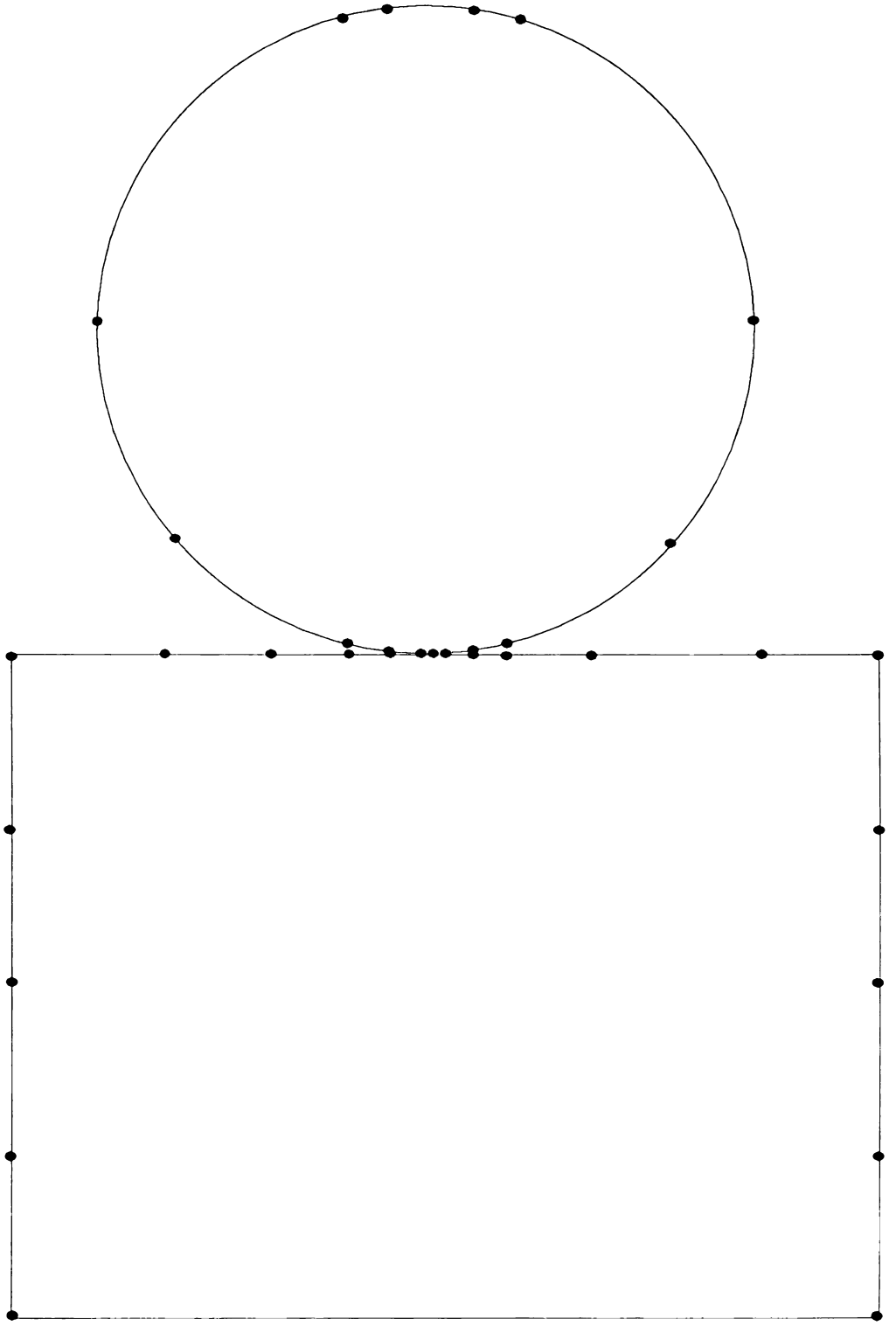

Figure IV.10
Model 2 example 2 (not to scale).

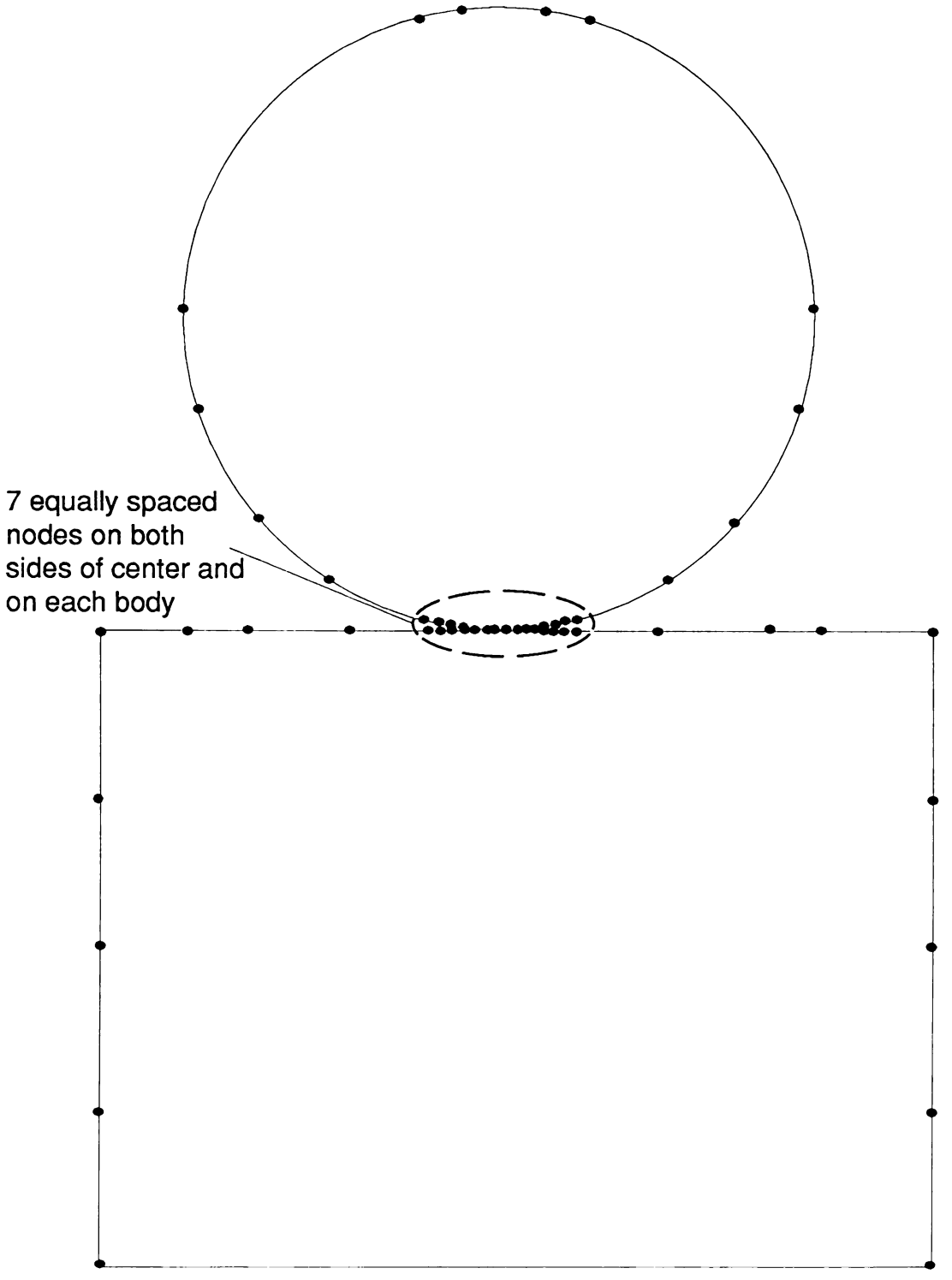

Figure IV.11
Model 3 example 2 (not to scale).

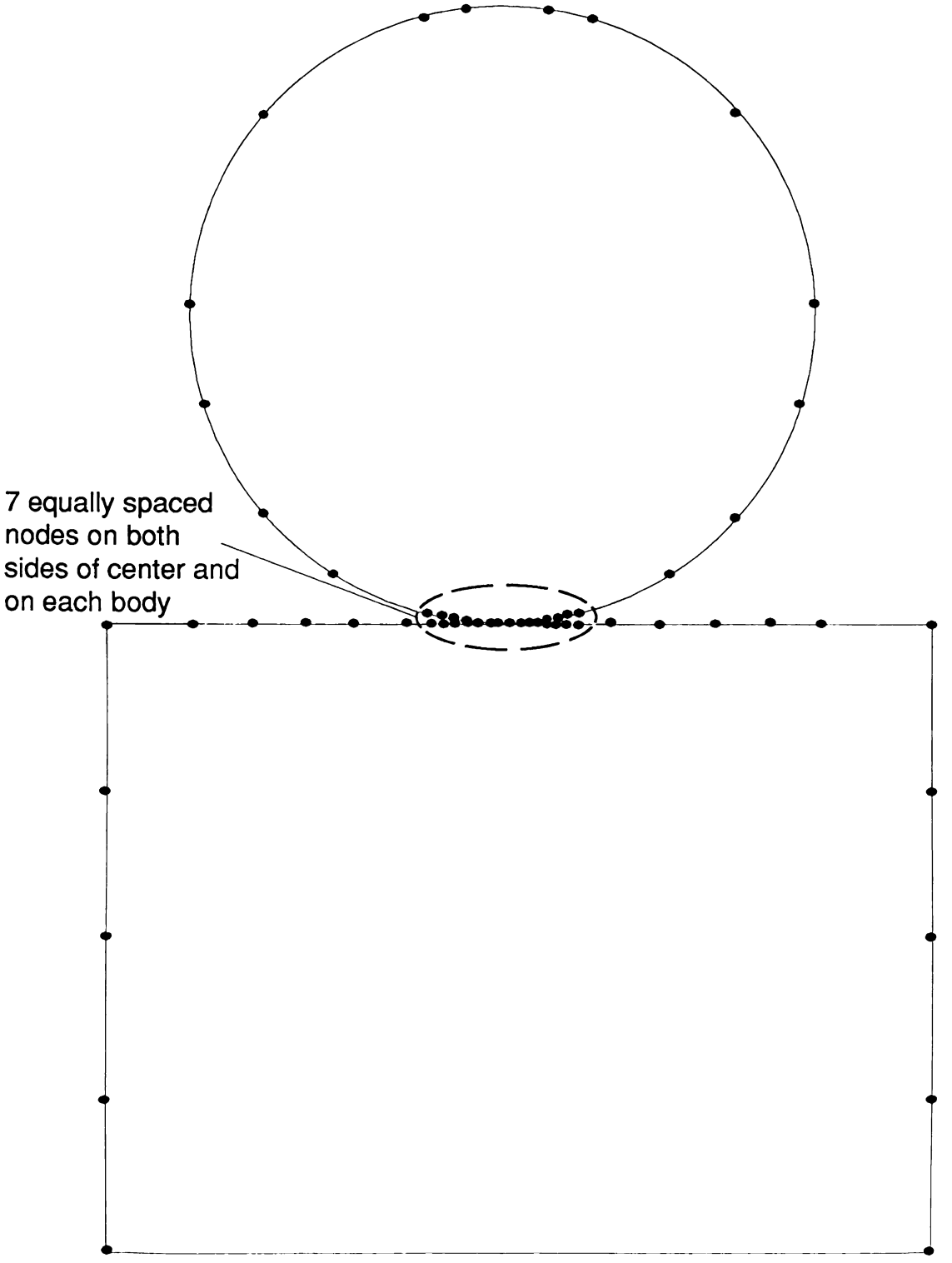

Figure IV.12
Model 4 example 2 (not to scale).

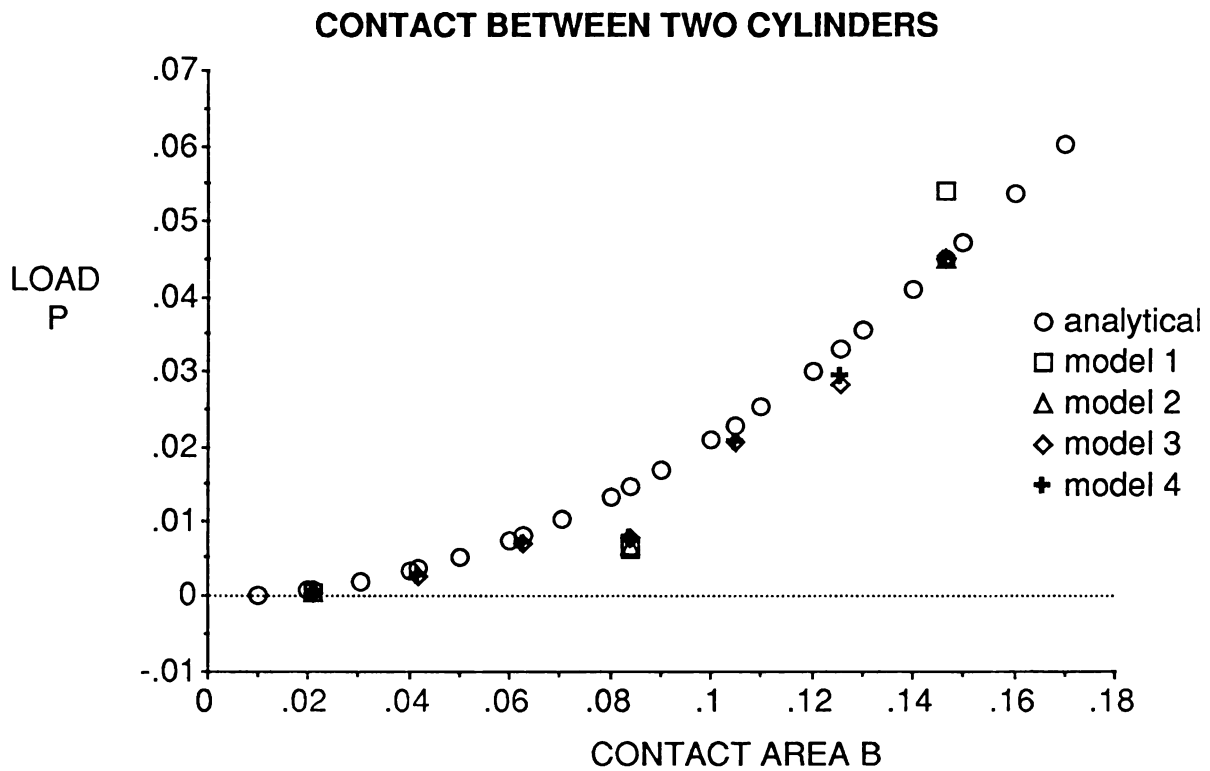

Figure IV.13
Contact area b versus externally applied load P for example 1.

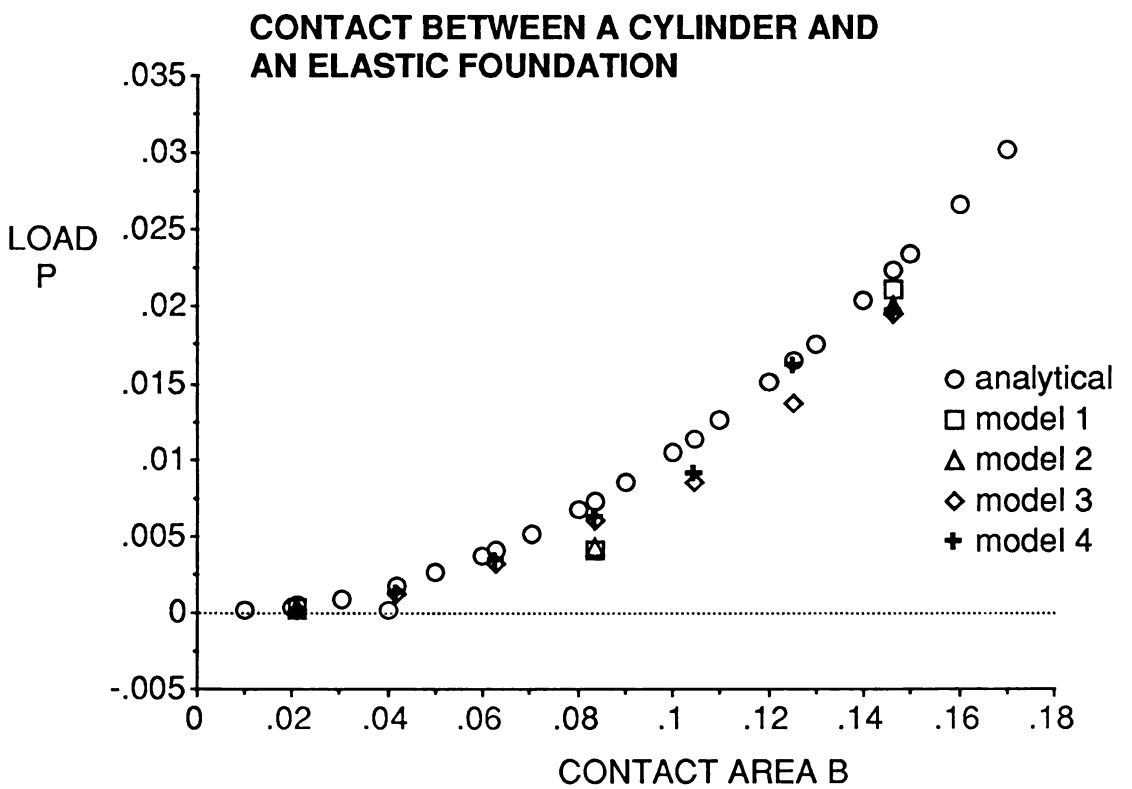

Figure IV.14
Contact area b bersus externally applied load P for example 2.

V.2 DISCUSSION OF RESULTS

From the two examples problems run, several things may be observed. The accuracy of results at any node, especially those near the contact region, are dependent on the element lengths in the vicinity of that particular node. This effect can be seen by looking at the results for the last contact point (b=.14658) for example 1. In model 1 the element lengths neighboring the last node are .02094 and .369618,respectively. The load P required to extend the contact area to include this node is .05398 which is greater than the analytically predicted result of .04487. In model 2 a node is added to reduce the larger element length. The element lengths neighboring the last node are now .02094 and .11512. The load P required to bring the last node into contact is .04504, which is a much better answer. In fact if another node was added, the load P required to bring the last node into contact would be reduced again. What can be seen from this is that the accuracy of results is highly sensitive to the mesh lenths surrounding that node.

The results for the first node in most cases considered deviated from the analytical values more than the values calculated for the other nodes in the contact region. This may be the result of having two large of a mesh size around the initial contact point. A better formulation may be to use a higher order interpolation function for both the tractions and displacements. This type of a formulation would allow the analyst to use a coarser mesh and still obtain accurate results

As the mesh was refined the results tended toward the analytical values. This type of trend would indicate that numerical values are converging as the mesh is

refinded. This property of convergence is very important as a test for the validity of numerical programs.

The boundary integral formulation produces ill-conditioned matrices, which cause numerical problems. The current solution technique used is a Guassian elimination procedure. Other techniques that are developed for ill-conditioned matrices should be sought to improve the accuracy of the analysis. Techniques to monitor the decomposition phase and report numerical accuracy loss, should also be implemented so that the analyst will know when numerical inaccuracies have occurred. This type of numerical problem will account for some of the discrepancies in the results presented.

In general, the procedure works well, but numerical aspects of the method need to be modified to provide more accurate results.

APPENDIX A

INFLUENCE FUNCTIONS

The influence functions for plane stress are as follows [18]:

$$(uR)_{ik} = [-(3-\nu)\delta_{ik}\log \rho + (1+\nu)q_iq_k]/(8\pi G)$$

$$(uc)_{11} = [2(1+\nu)(n_1q_1^3-n_2q_2^3) + (1-\nu)n_1q_1 + (3+\nu)n_2q_2]/(4\pi\rho)$$

$$(uc)_{12} = [2(1+\nu)(-n_2q_1^3-n_1q_2^3) + (1+3\nu)n_2q_1 + (3+\nu)n_1q_2]/(4\pi\rho)$$

$$(uc)_{21} = [2(1+\nu)(-n_2q_1^3-n_1q_2^3) + (3+\nu)n_2q_1 + (1+3\nu)n_1q_2]/(4\pi\rho)$$

$$(uc)_{22} = [2(1+\nu)(-n_1q_1^3-n_2q_2^3) + (1-\nu)n_2q_2 + 3 + \nu)n_1q_1]/(4\pi\rho)$$

$$(\sigma R)_{111} = [-2(1+\nu)q_1^3-(1-\nu)q_1]/(4\pi\rho)$$

$$(\sigma R)_{121} = [2(1+\nu)q_2^3-(3+\nu)q_2]/(4\pi\rho)$$

$$(\sigma R)_{221} = [2(1+\nu)q_1^3-(1+3\nu)q_1]/(4\pi\rho)$$

$$(\sigma R)_{112} = [2(1+\nu)q_2^3-(1+3\nu)q_2]/(4\pi\rho)$$

$$(\sigma R)_{122} = [2(1+\nu)q_1^3-(3+\nu)q_1]/(4\pi\rho)$$

$$(\sigma R)_{222} = [-2(1+\nu)q_2^3-(1-\nu)q_2]/(4\pi\rho)$$

$$(\sigma c)_{111} = G(1+\nu)[(1+4q_1^2-8q_1^4)n_1+2q_1q_2(1-4q_1^2)n_2]/(2\pi\rho^2)$$

$$(\sigma c)_{121} = G(1+\nu)[(1-8q_1^2q_2^2)n_2+2q_1q_2(1-4q_1^2)n_1]/(2\pi\rho^2)$$

$$(\sigma c)_{221} = G(1+\nu)[(1-8q_1^2q_2^2)n_1+2q_1q_2(1-4q_2^2)n_2]/(2\pi\rho^2)$$

$$(\sigma c)_{112} = (\sigma c)_{121}$$

$$(\sigma c)_{122} = (\sigma c)_{221}$$

$$(\sigma c)_{222} = G(1+\nu)[(1+4q_2^2-8q_2^4)n_2+2q_1q_2(1-4q_2^2)n_1]/(2\pi\rho^2)$$

where:

$$\rho = [(x_1-\zeta_1)^2 + (x_2-\zeta_2)^2]^{.5}$$

$$q_1 = (x_1-\zeta_1)/\rho \qquad q_2 = (x_1-\zeta_2)/\rho.$$

APPENDIX B

CALCULATION OF THE FREE TERM

The free term α'_{ij}, does not have to be calculated by solving the integral around the point of singularity. A relationship for the free term can be obtained by considering what will happen during a rigid body motion. Then from information already calculated during the analysis the free term is determined.

Recall that

$$[uc]G\{u\} = [uR]\{\mathbf{F}\}.$$

If we now look at this equation during a free body translation of an amount u_0 in the x and y directions, the following can be written,

$$\{\mathbf{F}\} = \{0\}$$

and

$$\{u\} = \{u_0\}.$$

The matrix form of the boundary integral equations can then be written as,

$$[uc]\{u_0\} = \{0\}.$$

This implies that

$$(uc)_{2n-1\ 2n-1} = -\sum_{\substack{m=1 \\ m\neq n}}^{N} (uc)_{2n-1\ 2m-1}$$

$$(uc)_{2n-1\ 2n} = -\sum_{\substack{m=1 \\ m\neq n}}^{N} (uc)_{2n-1\ 2m}$$

$$(uc)_{2n\ 2n-1} = -\sum_{\substack{m=1 \\ m\neq n}}^{N} (uc)_{2n\ 2m-1}$$

$$(uc)_{2n\ 2n} = -\sum_{\substack{m=1 \\ m\neq n}}^{N} (uc)_{2n\ 2m},$$

This means that the free term never has to be calculated directly, and the coefficient containing the free term is found by adding all the terms that multiple a displacement in the x or y direction, and taking the negative.

APPENDIX C

CALCULATION OF THE MEAN NORMAL

To define the local coordinate system of any set of nodal pairs a "mean normal" is defined. Each node is bounded by two elements on each side. Each element may have a different normal to the surface, see figure below.

Now the following is defined:

$$n_1 = \cos\theta,\ n_2 = \sin\theta,$$

$$n_{1f} = \cos\theta_f,\ n_{2f} = \sin\theta_f$$

and

$$n_{1s} = \cos\theta_s,\ n_{2s} = \sin\theta_s,$$

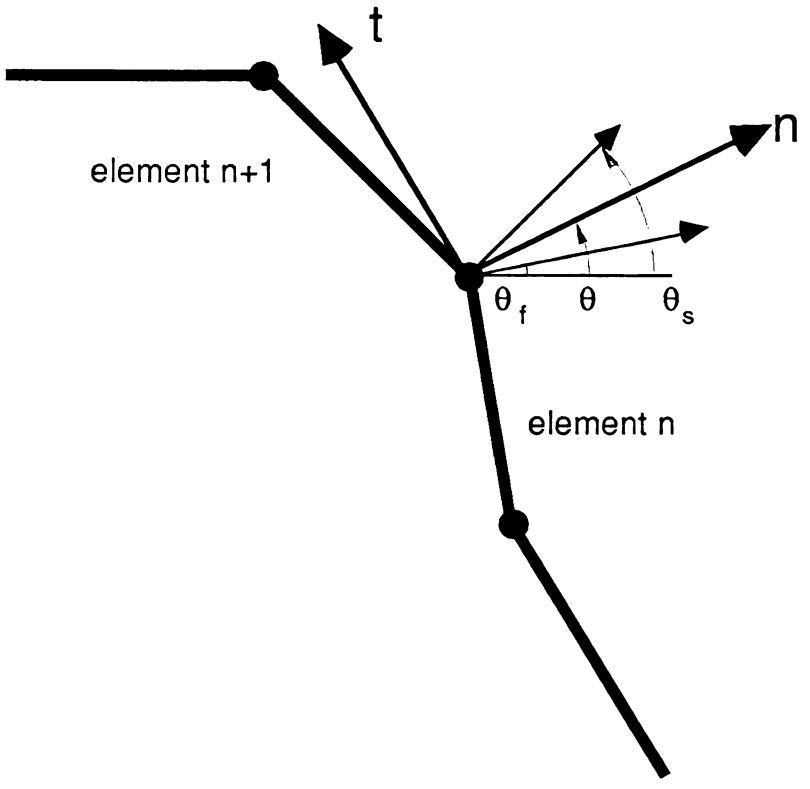

Figure C.1
Normals for an arbitrary node.

where

$\underline{n}_f$ = normal to element n,

$\underline{n}_s$ = normal to element n+1,

and

$$\underline{n} = .5(\underline{n}_f + \underline{n}_s)/|.5(\underline{n}_f + \underline{n}_s)|.$$

$$|.5(\underline{n}_f + \underline{n}_s)| = .5[(\cos\theta_f + \cos\theta_s)^2 + (\sin\theta_f + \sin\theta_s)^2]^{.5}$$
$$= .5[2 + 2(\cos\theta_f\cos\theta_s + \sin\theta_f \sin\theta_s)]^{.5}$$

$$\cos\theta = (\cos\theta_f + \cos\theta_s)/ [2 + 2(\cos\theta_f\cos\theta_s + \sin\theta_f \sin\theta_s)]^{.5}$$
$$\sin\theta = (\sin\theta_f + \sin\theta_s)/ [2 + 2(\cos\theta_f\cos\theta_s + \sin\theta_f \sin\theta_s)]^{.5}$$

Next consider a set of nodal pairs that are in contact, as seen below.

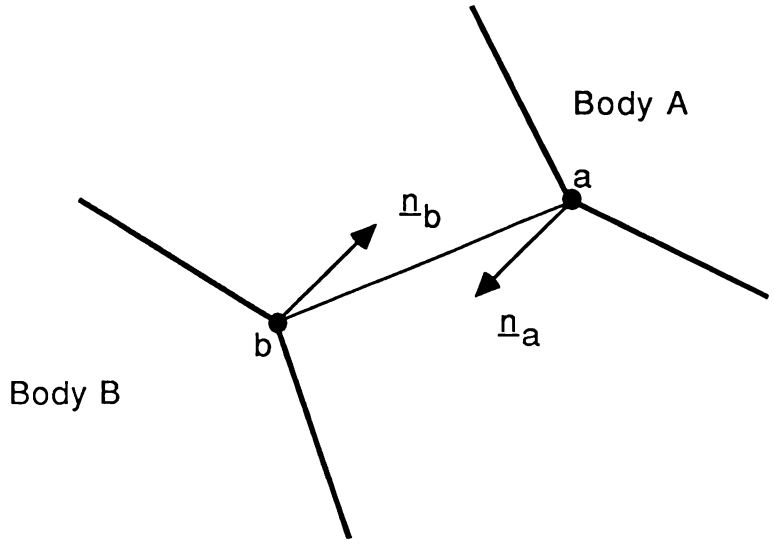

Figure C.2

Definition of the mean normal between nodal pairs a and b.

The "mean normal" from node a to node b, can now be defined as,

$$\underline{n}_m = .5(\underline{n}_a - \underline{n}_b)/|.5(\underline{n}_a - \underline{n}_b)|,$$

where

$$|.5(\underline{n}_a - \underline{n}_b)| = .5[(\cos\theta_a - \cos\theta_b)^2 + (\sin\theta_a - \sin\theta_b)^2]^{.5}$$

$$= .5[2 - 2(\cos\theta_a \cos\theta_b + \sin\theta_a \sin\theta_b)]^{.5}$$

and

$$\cos\theta_m = (\cos\theta_a - \cos\theta_b)/ [2 - 2(\cos\theta_a \cos\theta_b + \sin\theta_a \sin\theta_b)]^{.5}$$

$$\sin\theta_m = (\sin\theta_a - \sin\theta_b) / [2 - 2(\cos\theta_a \cos\theta_b + \sin\theta_a \sin\theta_b)]^{.5}$$

This defines the local coordinate normal and tangent to the surface of each body.

APPENDIX D

ORDER AND CONTINUITY OF TRACTIONS AND DISPLACEMENTS AT A BOUNDARY NODE

When developing the numerical formulation of the Boundary Element Method a choice of order and continuity of the traction and displacement functions must be made. What is meant here by choice of order is not whether the tractions and/or displacements will be simulated by constant, linear, or higher order functions, but will the tractions and displacement functions have the same order. The two choices are

1. both the tractions and displacements have the same order interpolation functions (constant, linear, ...),

2. the traction and displacement functions have a different order (constant tractions and linear displacements).

First consider the case where the interpolation functions are of the same order (both constant, linear, quadratic, ...). To have a square system of equations (square meaning the same number of unknowns as equations) the continuity conditions must be the same at each node. That is, both the traction and displacement components are either continuous or discontinuous. The problem with a discontinuous formulation is that a discontinuity of displacement at a node means that a node would have to split because the displacement on each side of that node is multi-valued. This does not simulate a continuous medium well. The more common formulation found in most industry standard programs uses a continuous traction and displacement formulation. In industry this is known as an isoparametric formulation. The problem with this formulation is that at the corners of a model a node is multi-valued. To simulate the corner these programs place two nodes very close to each other. This takes care of the multi-valued traction problem but is not a true representation of the actual problem being

simulated. A second problem with this type of formulation is that most load model loading is discontinuous. That is a load is concentrated over a prescribed area and everywhere else is zero. This poses another problem for this type of formulation.

Instead of choosing the displacement and traction functions to be of the same order, one may chose the displacement functions to be an order lower than the order of the traction functions. In order to have a square system of equations for this formulation the displacement must be discontinuous and the tractions must be continuous. This type of a procedure has two problems. As stated above a discontinuous displacements formulation causes problems simulating a continuous medium. Also, continuous traction formulations have to have special procedures for corners and discontinuous loading. The other choice for order of the traction and displacement functions is to allow the displacement functions to be one order higher than the traction functions. A square system of equations may be obtained for this formulation with continuous displacements and discontinuous tractions.

APPENDIX E

SINGULAR INTEGRALS

The singular integrals are evaluated analytically while all other nonsingular integrals are evaluated by numerical integration. The integrals become singular when the element begins or ends with the node n (see Figure E.1).

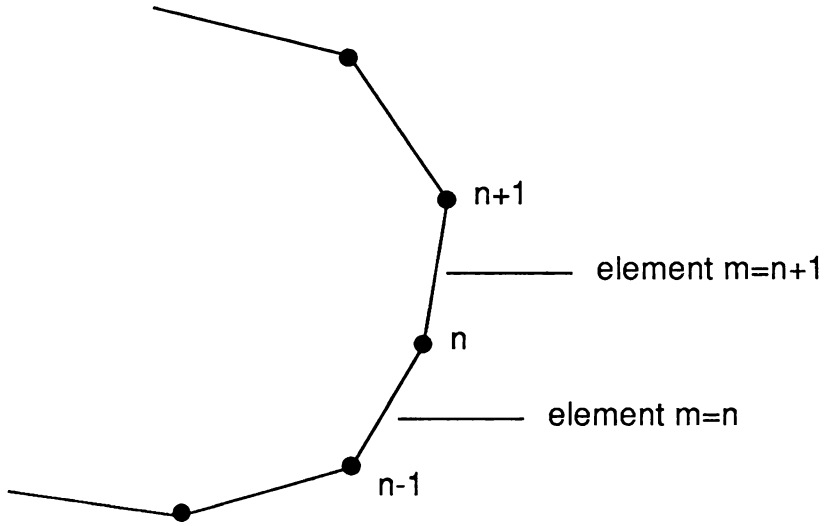

Figure E.1
Partial diagram of the boundary showing the boundary elements with singular considerations.

The contributions from the singular integrals are as follows:

$$A_{11}^{n\,n} = A_{11}^{n+1\,n} = B_{11}^{n\,n} = B_{11}^{n+1\,n} = 0$$

$$A_{22}^{n\,n} = A_{22}^{n+1\,n} = B_{22}^{n\,n} = B_{22}^{n+1\,n} = 0$$

$$A_{12}^{n\,n} = -A_{21}^{n\,n} = (1-\nu)/2\pi$$

$$B_{12}^{n+1\,n} = -B_{21}^{n+1\,n} = -(1-\nu)/2\pi$$

$$A_{12}^{n+1\,n} + B_{12}^{n\,n} = A_{21}^{n+1\,n} + B_{21}^{n\,n} = ((1-\nu)/2\pi)\log(\Delta s_n/\Delta s_{n+1})$$

BIBLIOGRAPHY

BIBLIOGRAPHY

1. Hertz, H., miscellaneous papers -On The Contact Of Elastic Solids (translated by D. E. Jones) Macmillan, London, (1896).

2. C. Lipson and R. C. Juvinall, Handbook of Stress and Strength, Macmillan, New York (1963).

3. ABAQUS, Example Problems Manual, Hibbitt, Karlsson and Sorensen, Inc., Version 4.5, (1982).

4. Fredriksson, B., Finite Element Solution of Surface Nonlinearities in Structural Mechanics With Special Emphasis to Contact and Fracture Mechanics Problems, Computers & Structures, 6, 281-290 (1976).

5. Mahmoud, F. F., Salamon, N. and Marks, W. R., A Direct Automated Procedure for Frictionless Contact Problems, International Journal For Numerical Methods In Engineering, 18, 245-257 (1980).

6. Mazurkieewicz, M., Ostachowicz, W., Theory of Finite Element Method For Elastic Contact Problems Of Solid Bodies, Computers & Structures, 1, 51-59 (1983).

7. Torstenfelt, B., Contact Problems With Friction in General Purpose Finite Element Computer Programs, Computers & Structures, 16, 487-493 (1983).

8. Torstenfelt, B., An Automatic Increment Technique for Contact Problems with Friction, Computers & Structures, 19, 393-400(1984).

9. Rahman, M. U., Rowlands, R. E., Cook, R. D., Wilkinson, T. L., An Iterative Procedure for Finite-Element Stress Analysis of Frictional Contact Problems, Computers & Structures, 18, 947-954 (1984).

10. Rizzo, F. J., An Integral Equation Approach to Boundary Value Problems Of Classical Elastostatics, 83-95 (1965).

11. Rizzo, F. J., The Boundary-Integral Equation Method: A Modern Computational Procedure in Applied Mechanics, 1-5 (1975).

12. Andersson, T., The Boundary Element Method Applied To Two-Dimensional Contact Problems With Friction, Proceedings of the Third International Seminar, Irvine, California, July 1981, Ed. C. A. Brebbia, Springer-Verlag, Berlin.

13. Andersson, T., The Second Generation Boundary Element Contact Program, Proceedings of the Fourth International Seminar, Southhampton, England, September 1982, Ed. C. A. Brebbia, Springer-Verlag, Berlin.

14. Abdul-Mihsein, M. J., Bakr, A. A. and Parker, A. P., A Boundary Integral Equation Method For Axisymmetric Elastic Contact Problems, Computers & Structures, 23, 787-793 (1986).

15. Kalker, J. J., On Elastic Line Contact, Journal of Applied Mechanics, 3,1125-1132 (l972).

16. Banerjee, P. K. and Butterfield, R., Boundary Element Methods In Engineering Science, McGraw Hill Book Co.,London, (1981).

17. Press, W. H., Flannery, B. P., Teukolsky, S. A. and Vetterling, W. T., Numerical Recipes The Art of Scientific Computing, Cambridge University Press, Cambridge, (1987).

18. Garcia, J. J., Coupling of the Finite Element and Boundary Element Methods for the Solution of Plane Problems of Linear Elasticity, M.S. Thesis, Department of Metallurgy, Mechanics and Materials Science, Michigan State University (1984).

19. Timoshenko, S. P. and Goodier, J. N., Theory of Elasticity, McGraw Hill Book Co., New York (1953).

20. Wang, C. Applied Elasticity, McGraw-Hill, New York, (l953).

21. Cook, R. D., Concepts and Applications of Finite Element Analysis, John Wiley and Sons, New York (1974).

22. Altiero, N., Gauazza, On a Unified Boundary Integral Equation Method, Journal of Elasticity,10, 1-9 (1980).